Resource dependency and communication networks in Early Neolithic western Europe

Michael Kempf, Solène Denis

Quaternary Environments and Humans 2 (2024) 100014

Contents lists available at ScienceDirect

Quaternary Environments and Humans

journal homepage: www.journals.elsevier.com/quaternary-environments-and-humans

Resource dependency and communication networks in Early Neolithic western Europe

Michael Kempf[a,*,1], Solène Denis[b,2]

[a] Quaternary Geology, Department of Environmental Sciences, University of Basel, Bernoullistrasse 32, Basel 4056, Switzerland
[b] CNRS, UMR 8068 TEMPS, MSH Mondes, Bâtiment René Ginouvès, 21 allée de l'Université, Nanterre Cedex 92023, France

ARTICLE INFO

Handling Editor: Dr Kolář Jan

Keywords:
Computational archaeology
Network analysis
Spatial modelling
Least Cost Path analysis
Lithic technology

ABSTRACT

During the European Neolithisation Process, a pivotal facet of Neolithic population dynamics lay in the capability of agro-pastoral communities to procure high-quality raw material for stone tools. Whether this material was sourced from local geological units or got transported via large-scale communication networks is, however, not yet fully understood. To trace the distribution patterns of Early Neolithic resource dispersal, we present a multicomponent network analysis and the first resource dependency model of Middle Eocene lithic records across western Europe. The model builds on topographic landscape permeability and Bartonian silicite dispersal and estimates the Chaine Operatoire (CO) sequences from i) directly sourced raw material based on accumulative cost functions; ii) chronologically differentiated network models; iii) a probability model of potential site distributions based on a point process model (PPM). We resume that early Neolithic site locations were particularly targeted at connecting to the supraregional resource exchange network that originated from the Paris Basin. Local resource exploitation predominated in the core region of Bartonian silicite distribution whereas distant sites were located on or close to high-probability communication and network corridors. Particularly striking is the differentiation highlighted by the CO segmentation towards the end of the Early Neolithic with distinct patterns of clustered production, intermediate, and dispersed consumer sites. This indicates that major production centres can be expected in close distance to the resource with high consumer density in secondary centres in a star-shaped pattern across the study area.

1. Introduction

It is assumed that the neolithisation of Europe follows two major roads, a Mediterranean coastal pathway and a continental direction along the river Danube. The LBK (Linear Pottery Culture) is mainly at the roots of the Central and north-western Europe neolithisation process between around 5400–5050 BCE. On its western fringe, it reaches the Paris Basin, Normandy and the margins of Brittany (Fig. 1). At the turn of the 5th millennium BCE, the dissolution of the European LBK led to a cultural recomposition characterised in particular by a form of regionalization (see, for example, Hamon and Manen, 2021). It has furthermore been suggested by Furholt (2018) that this phenomenon could reflect a decline in the spatial scale of mobility networks. The parameters that controlled these mobility networks and the spatial scales on which communication and exchange took place, however, are yet not well understood. The transformation of Neolithic mobility networks has not been tested against spatial or environmental data to detect potential causality between site distribution, resource dispersal, topographic elements or chronological development of the production CO during the Neolithic period in wwestern western Europe.

This article presents the first comprehensive network and resource dependency model for the western European Early Neolithic based on multivariate environmental input variables. We focus on a well-defined post-LBK group, the Blicquy/Villeneuve-Saint-Germain (BVSG) cultural complex. This chrono-cultural group emerged in the Paris Basin around 5000 BCE before spreading from Brittany to eastern Belgium and from North France to the Loire river valley. Archaeological observations have revealed a more varied occupation of the landscape than for the LBK,

* Corresponding author.
E-mail addresses: michael.kempf@unibas.ch (M. Kempf), solene.denis@cnrs.fr (S. Denis).
[1] ORCID: 0000–0002-9474–4670
[2] ORCID: 0000–0001-7986–217X

https://doi.org/10.1016/j.qeh.2024.100014
Received 6 March 2024; Received in revised form 10 June 2024; Accepted 14 June 2024
Available online 27 June 2024

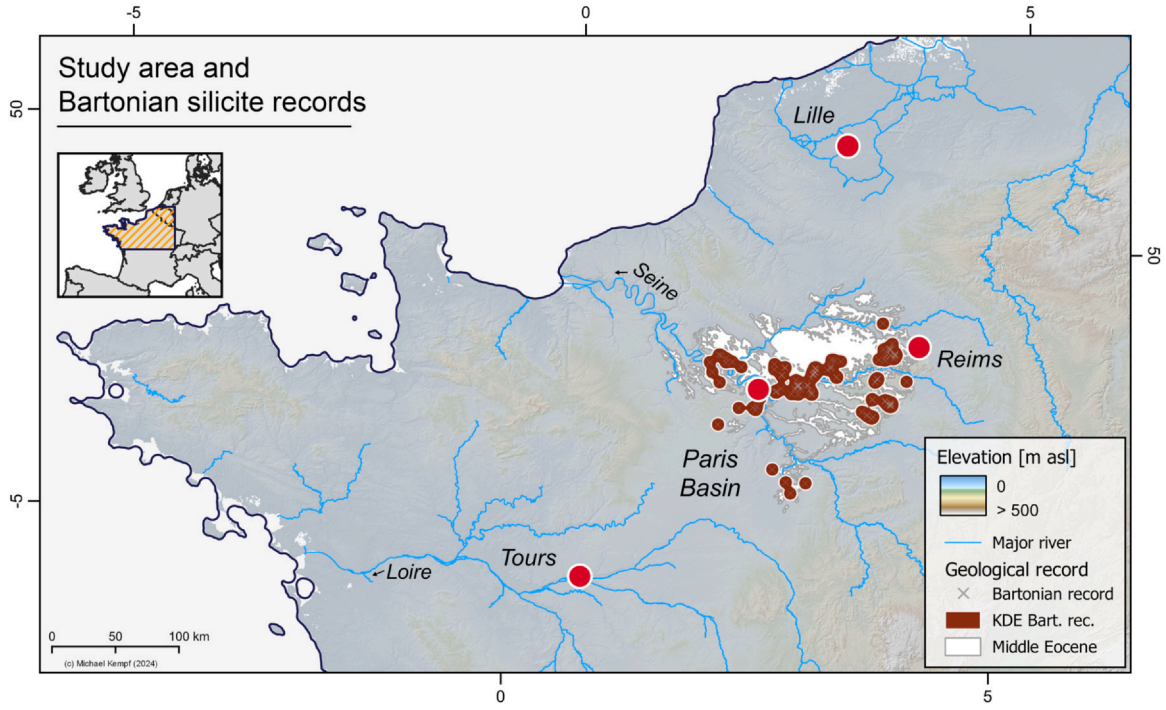

Fig. 1. Study area and distribution of Bartonian silicite density distribution in western Europe. Bartonian silicite record are visualised as a Kernel Density Estimation (KDE Bart. rec.). Major modern cities are marked with red dots. Bartonian silicite resources are mostly distributed in the Paris Basin. Database of Bartonian outcrops from the Collective Research Project *Matières premières du Bassin parisien* (Allard, 2022).

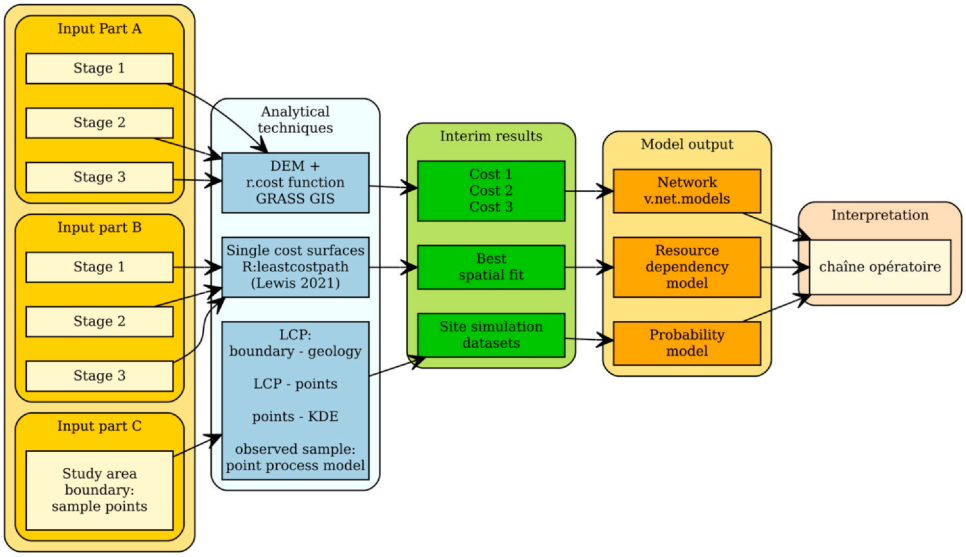

Fig. 2. Outline of the methodical and analytical workflow of this paper. Starting from left: input data (yellow boxes); analytical techniques (blue boxes); interim results (green boxes); model output (orange boxes); interpretation (right box).

especially during the middle and late stages. Seriation of pottery decoration led to the division of this large cultural complex into three stages (Constantin, 1985) (early, middle and late, hereafter named stage 1, stage 2 and stage 3), spanning from 5000/4950–4750/4650 BCE (Dubouloz, 2003). More recent seriations focused on certain sites or micro-regions validated this division, while at the same time clarifying certain regional sequences (Bostyn et al., 2003; Hauzeur, 2008; Lanchon, 2008). This tripartition can be corroborated by lithic studies (Allard and Bostyn, 2006; Denis, 2019), livestock farming (Bedault and Hachem, 2008) or the characteristics of adornments (Bonnardin, 2009; Fromont et al., 2008). The quantity of available radiocarbon dates does not yet allow us to propose an absolute chronology for these three stages. However, recent work on VSG dates in northern France suggests a stage 2 around 4900–4850 BCE and a middle date for the stage 3 around 4750 cal BC (Praud et al., 2018).

In the presented approach, we use these three stages to test against topographically determined movement corridors, chronological network models as well as potential resource dependencies and supply chains that potentially control site distribution patterns across Early Neolithic France and Belgium. We hypothesise the close link between environmentally controlled movement corridors and socio-culturally established communication networks. We aim at creating a set of multiple explanatory models to recognize site distribution patterns and to understand the complex interplay of material resourcing, production, and consumption across different chronological stages.

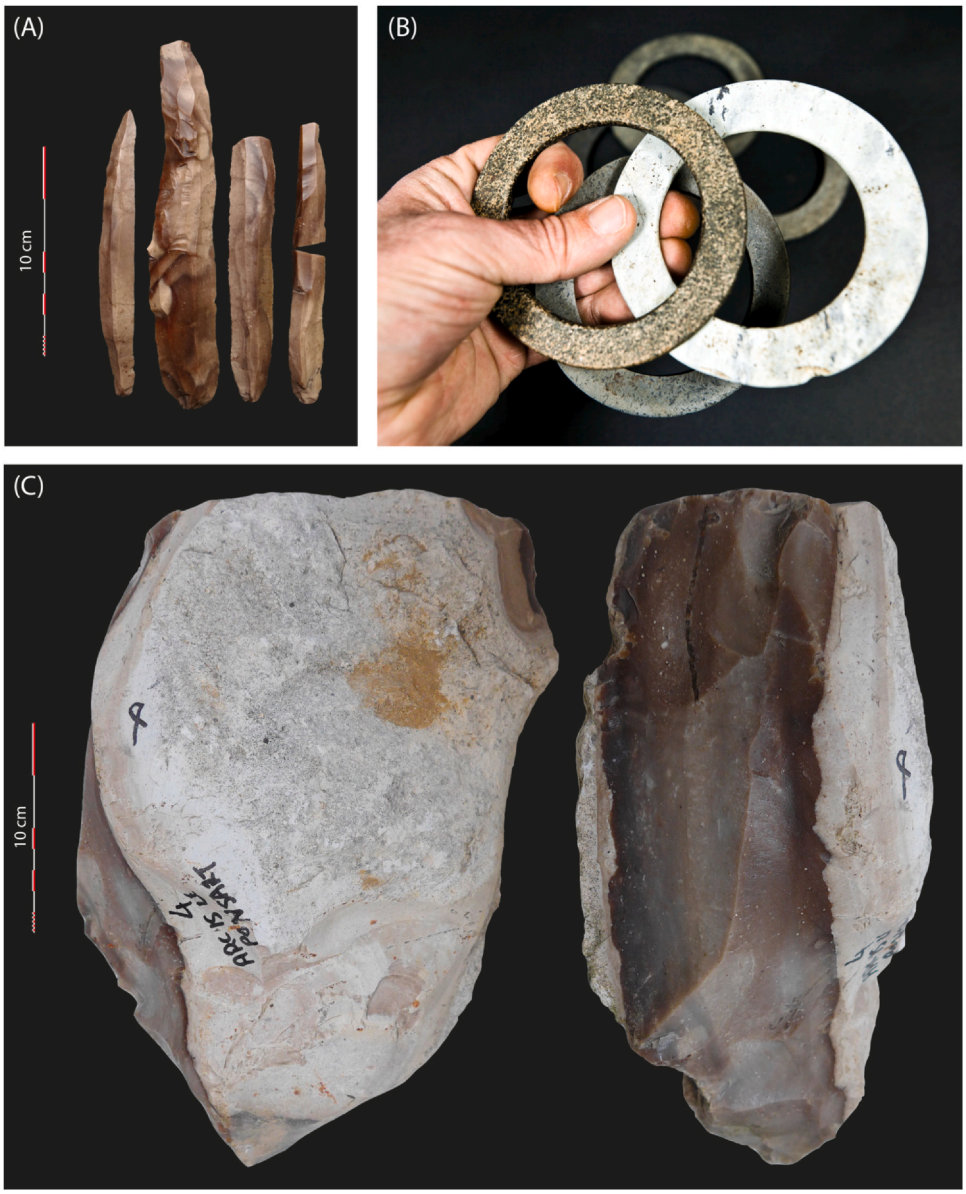

Fig. 3. Elements considered as identity markers for the BVSG populations. Left: fragments or long blades made from Bartonian silicite from the Paris Basin discovered at the Belgian BVSG sites (image credits: Solène Denis); right: bracelets made from schist and serpentinite originating from the site of Presles-et-Boves, Aisne valley (France) (image credit: François-Xavier Dessirier, Aisne Department). Bottom: block of Bartonian silicite from raw material surveys in Arcis-le-Ponsart, Marne (image credit: Pierre Allard).

To explore our hypotheses, the paper is methodologically structured as follows: (i) we evaluate the distance relationship between all sites and the closest resource availability based on energy expenditure to reach the resource; (ii) a comprehensive chronological network analysis based on topography that connects all sites in each stage into a complete network approach; (iii) using all sites of all stages and a point process model of complete landscape permeability and resource dispersal, we create a probability model of potential site distribution compared to the covariates topography and resource. The network, the resource dependency model, and the probability distribution is then compared to the archaeologically suggested CO of the main Bartonian silicite raw material circulation network in the study area.

We present a fully reproducible and replicable workflow written in the R programming language (R Core Team (2021) that allows the comparison to different regions and chronological periods and enables a cross-regional evaluation of Neolithic site distributions in future scientific approaches.

2. Material and methods

Using a variety of modelling approaches, this paper aims at detecting spatial patterns in archaeological site distribution compared against geological and topographical parameters (Fig. 2). In the first paragraphs of this section, we describe the archaeological site database and the underlying material culture and chronological differentiation followed by the environmental settings of the study area. Then, we introduce the general network model approach of the paper following the *v.net.models* algorithm in GRASS (GRASS Development Team, 2020)) presented in Ducke and Suchowska (2022). Following that, we formulate the resource dependency model of each chronological stage related to the distribution of Bartonian silicite. Building on accumulative Least Cost Path analyses, we present a workflow for a probability model of the entire study area in relation to resource accessibility. Lastly, we compare the models and the site distribution and networks to the locally and regionally diverse CO segmentation of the lithic material

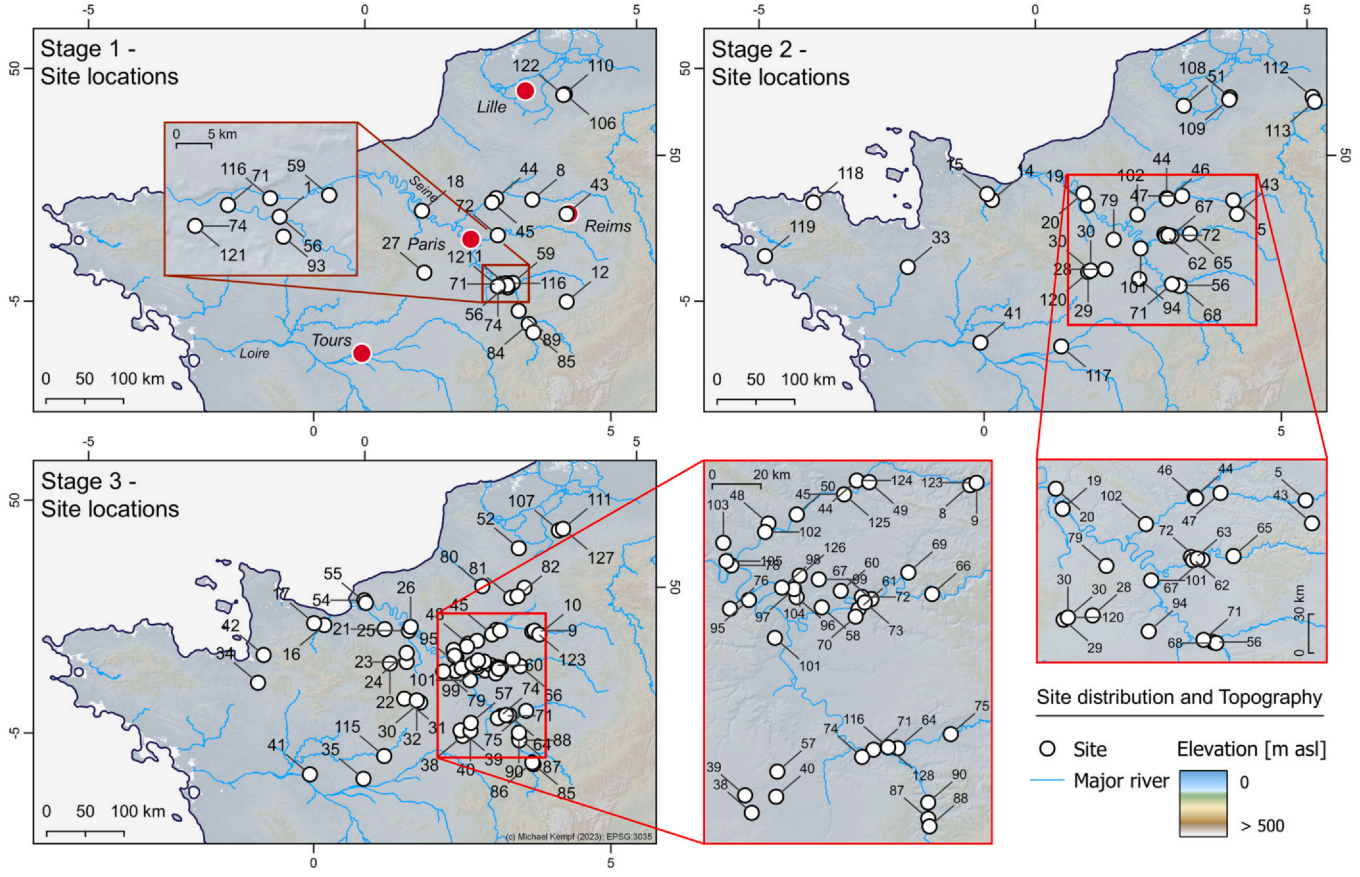

Fig. 4. Site location and IDs of the three Early Neolithic samples used in the analysis (see Table 1 in the repository for site ID and context information).

culture in western Europe. Movement corridor models, resource dependencies, and statistical analyses were conducted using R software and the following packages: *leastcostpath* (Lewis, 2023a), sf (Pebesma, 2018; Pebesma and Bivand, 2023), terra (Hijmans, 2023), spatstat (Baddeley et al., 2015). All code and auxiliary datasets and packages to this article are available from https://zenodo.org/records/11165502 and https://zenodo.org/records/10617484.

2.1. Study area

The study area's window of operation stretches from central and northern France towards Belgium, including parts of Luxemburg and the Netherlands (Fig. 1). The archaeological dispersal, however, is limited to Belgium and France (see Section 2.2). We chose a larger window to avoid edge effects during the statistical spatial analysis. Topographic situation in the study area changes quite dramatically from the South East Alpine region (> 4000 m asl) towards the rather even and low-lying Champagne plain in the centre of France, the Paris Basin (with elevation ranges of approximately 100–250 m asl), and to the western boundaries of the French shoreline in Normandy and Brittany. The topographic change is mirrored in the hydrologic systems draining the Alps and the Alpine foreland, the northern Morvan region to the Atlantic coast and the Channel in the North. The riverbed dynamics change accordingly from an erosive to a sedimentary character, accumulating massive deposits on top of largely Mesozoic geological units of the central plain. The chronostratigraphical boundary from the Mesozoic to the Cenozoic is then of particular interest to this study as it holds the Eocene-dating Bartonian silicite records (Fig. 3) that are dispersed across the Paris Basin in between the rivers Marne and Oise in the north and the river Seine to the south (Allard, 2022).

2.2. Archaeological data

The analysis relied on the comparison between the three chronological stages to understand the evolution of the network organisation. This implied the construction of a dataset building on "clearly dated" sites. Hence, we excluded those sites that were not attributed to any precise chrono-cultural stages of the BVSG. This bias could for example be related to a low number of pottery, a non-specific assemblage, or missing in-depth analysis. Furthermore, we only took into account the sites for which lithic research information and the determination of siliceous raw material were available. Parts of the database build on the research undertaken by Bostyn et al. (2019) and were extended and completed by the overview of the lithic CO segmentation, essentially based on literature review and previous approaches by the authors (Denis, 2012). The database now consists of n = 22 sites for stage 1, n = 36 sites for stage 2 and n = 75 sites for stage 3 (Fig. 4; see Table 1 in the repository to this article). The increasing sample sizes in stage 2 and 3 reflect an empirically observed density with (i) an extended topographical occupation (e.g. the high terraces of the river valleys) and (ii) the occupation of marginal regions such as Brittany or the tributary valleys (Bostyn and Lanchon, 2007), rather than a research intensity bias.

Compared to the LBK culture in northern France and Belgium, the BVSG distinguished itself particularly by two elements that were qualified as so-called identity markers (Allard and Bostyn, 2006; Bostyn, 2008; Fromont, 2013): schist bracelets (Fig. 3, below, right panel) and long blades made from Bartonian silicite (Fig. 3, below, left panel).

The source of the raw material is located in a particular geographical area characterising the broader extent of the BVSG dispersal. Schist outcrops originate from two distinct locations: the Armorican Massif in the north-west of France and the Ardennes mountain range at the border of eastern France to Belgium (Burnez-Lanotte et al., 2005;

Table 1
Site names, location, and attributes of the sample used during the analysis. Sites are organised according to stage dependency. Coordinates are in WGS84, EPSG:4326.

id	Commune	Lat	Lon	Stage 1	Stage 2	Stage 3	Bartonian silicite	Sequence CO
1	Barbey	48.3647	3.055695	X			1	3
8	Villeneuve-Saint-Germain	49.379923	3.359372	X		X	1	NA
12	Buchères	48.23564	4.11022	X			0	0
18	St-Pierre d'Autils	49.118648	1.433717	X			0	0
27	Sours	48.4115	1.597002	X			0	0
43	Tinqueux	49.247881	3.985803	X	X		1	1
44	Longueil-Sainte-Marie	49.357706	2.717882	X	X	X	1	2
45	Pontpoint	49.302169	2.65402	X		X	1	1
56	Barbey	48.364654	3.055692	X	X		1	2
59	Balloy	48.39826	3.147072	X			1	2
71	Varennes-sur-Seine	48.373328	2.954487	X	X	X	N/A	N/A
72	Vignely	48.93141	2.810012	X	X	X	1	2
74	Ville-Saint-Jaques	48.342624	2.89537	X		X	0	0
84	Charmoy	47.940158	3.48884	X			N/A	N/A
85	Monéteau	47.848219	3.579423	X		X	0	0
89	Villeneuve-sur-Yonne	48.082084	3.294212	X			0	0
93	Villeneuve-la-Guyard	48.339739	3.066428	X			0	0
106	Ath	50.630813	3.777105	X			1	2
110	Irchonwelz	50.620105	3.753837	X			1	2
116	Marolles	48.38722	3.034237	X		X	1	2
121	Ville-Saint-Jaques	48.342626	2.89539	X		X	N/A	N/A
122	Irchonwelz	50.62011	3.753838	X			1	2
id	**Commune**	**Lat**	**Lon**	**Stage 1**	**Stage 2**	**Stage 3**	**Bart.**	**C. O.**
5	Berry-au-Bac	49.403135	3.900199		X		1	2
14	Fontenay-le-Marmion	49.093441	-0.351945		X		0	0
15	Verson	49.155552	-0.450904		X		1	3
19	Aubevoye	49.174295	1.334829		X		1	3
20	Poses	49.307801	1.238889		X		1	3
28	Auneau	48.46299	1.775277		X		0	0
29	Barjouville	48.409897	1.479147		X		0	0
30	Chartres	48.428856	1.520528		X		0	0
30	Chartres	48.428856	1.520528		X	X	0	0
33	Betton	48.181652	-1.641428		X		0	0
41	Beaufort-en-Vallée	47.43997	-0.215973		X	X	0	0
43	Tinqueux	49.247881	3.985803	X	X		1	1
44	Longueil-Sainte-Marie	49.357706	2.717882	X	X	X	1	2
46	Rivecourt	49.347972	2.735113		X		1	1
47	Trosly-Breuil	49.401089	2.98824		X		1	4
51	Loison-sous-Lens	50.442479	2.862387		X		1	3
56	Barbey	48.364654	3.055692	X	X		1	2
62	Fresnes-sur-Marne	48.937964	2.740038		X		1	1
63	Jablines	48.917444	2.764653		X		1	4
65	Luzancy	48.972976	3.187112		X		1	1
67	Mareuil-lès-Meaux	48.926631	2.863522		X	X	1	1
68	Misy-sur-Yonne	48.35961	3.089536		X		NA	NA
71	Varennes-sur-Seine	48.373328	2.954487	X	X	X	1	3
72	Vignely	48.93141	2.810012	X	X	X	1	2
79	Neauphle-le-Vieux	48.815028	1.862389		X	X	1	2
94	Maisse	48.394151	2.375605		X		1	3
101	Rungis	48.748323	2.347192		X	X	1	1
102	Champagne-sur-Oise	49.13379	2.231572		X	X	1	3
108	Blicquy	50.587687	3.685799		X		1	2
109	Ellignies-Sainte-Anne	50.561297	3.677118		X		1	2
112	Darion	50.664895	5.187166		X		1	3
113	Vaux-et-Borset	50.613169	5.231593		X		1	2
117	Onzain	47.515923	1.165476		X		0	0
118	Lannion	48.731646	-3.453774		X		0	0
119	Quimper	48.018527	-4.113472		X		0	0
120	Chartres	48.42887	1.52055		X		0	0
id	**Commune**	**Lat**	**Lon**	**Stage 1**	**Stage 2**	**Stage 3**	**Bart.**	**C. O.**
8	Villeneuve-Saint-Germain	49.379923	3.359372	X		X	1	1
9	Bucy-le-Long	49.391357	3.39467			X	1	1
10	Vasseny	49.353264	3.487199			X	1	2
11	Vermand	49.876691	3.150399			X	1	3
16	Mondeville	49.176919	-0.320048			X	1	3
17	Saint-Manvieu-Norrey	49.181702	-0.50326			X	0	0
21	Bosrobert	49.22357	0.752763			X	0	0
22	Breteuil-sur-Iton	48.836355	0.916101			X	0	0
23	Chavigny-Bailleul	48.875652	1.204329			X	0	0
24	Guichainville	48.979852	1.186959			X	0	0
25	Incarville	49.238925	1.178932			X	1	3
26	Léry	49.285749	1.203014			X	1	3
30	Chartres	48.428856	1.520528		X	X	0	0
31	Courville-sur-Eure	48.450276	1.238747			X	1	3

(*continued on next page*)

Table 1 (*continued*)

id	Commune	Lat	Lon	Stage 1	Stage 2	Stage 3	Bartonian silicite	Sequence CO
32	Mainvilliers	48.448909	1.458083			X	0	0
34	Saint-Etienne-en-Coglès	48.403222	-1.326796			X	0	0
35	Chanceaux-sur-Choisille	47.471202	0.703314			X	0	0
38	Courcelles-le-Roi	48.096308	2.317858			X	0	0
39	Dadonville	48.157911	2.270984			X	0	0
40	Echilleuses	48.16471	2.442809			X	1	3
41	Beaufort-en-Vallée	47.43997	-0.215973		X	X	0	0
42	Plomb	48.730722	-1.302604			X	0	0
44	Longueil-Sainte-Marie	49.357706	2.717882	X	X	X	1	2
45	Pontpoint	49.302169	2.65402	X		X	1	1
48	Chambly	49.166157	2.244947			X	1	2
49	Lacroix-Saint-Ouen	49.35608	2.789233			X	1	1
50	Villers-sous-Saint-Leu	49.210343	2.399125			X	1	2
52	Vitry-en-Artois	50.325931	2.980959			X	0	0
54	Saint-Aubin-Routot	49.524001	0.325571			X	1	3
55	Saint-Vigor-d'Ymonville	49.495472	0.359794			X	0	0
57	Boulancourt	48.25761	2.435464			X	1	3
58	Chelles	48.878272	2.591082			X	1	1
60	Claye-Souilly	48.945794	2.688632			X	1	2
61	Coupvray	48.88429	2.797088			X	1	1
64	La Tombe	48.387503	3.089027			X	NA	NA
66	Méry-sur-Marne	48.966671	3.201057			X	1	2
67	Mareuil-lès-Meaux	48.926631	2.863522		X	X	1	2
69	Ocquerre	49.03759	3.056944			X	1	4
70	Serris	48.856611	2.785638			X	NA	NA
71	Varennes-sur-Seine	48.373328	2.954487	X	X	X	1	3
72	Vignely	48.93141	2.810012	X	X	X	1	1
73	Villenoy	48.912107	2.828659			X	1	2
74	Ville-Saint-Jaques	48.342624	2.89537	X		X	1	3
75	Villiers-sur-Seine	48.457008	3.374325			X	0	0
76	Bailly	48.83798	2.080186			X	1	3
78	Maurecourt	48.99745	2.062523			X	1	4
79	Neauphle-le-Vieux	48.815028	1.862389		X	X	1	1
80	Boves	49.846258	2.393408			X	1	3
81	Languevoisin-Quiquery	49.747423	2.930153			X	1	3
82	Sancourt	49.77263	3.040508			X	0	0
85	Monéteau	47.848219	3.579423	X		X	0	0
86	Gurgy	47.866609	3.558284			X	0	0
87	Etigny	48.138165	3.291157			X	1	3
88	Passy	48.110266	3.302088			X	1	3
90	Sens	48.197722	3.282798			X	1	3
95	Rueil-Malmaison	48.877654	2.180333			X	1	3
96	Bobigny	48.906322	2.44541			X	1	2
97	Le Bourget	48.935106	2.426241			X	1	2
98	Saint-Denis	48.935687	2.357842			X	1	2
99	Tremblay-en-France	48.980124	2.559061			X	1	NA
101	Rungis	48.748323	2.347192		X	X	1	1
102	Champagne-sur-Oise	49.13379	2.231572		X	X	1	3
103	Courcelles-sur-Viosne	49.077554	2.003669			X	1	2
104	Gonesse	48.986243	2.450112			X	1	2
105	Jouy-le-Moutier	49.011343	2.031278			X	NA	NA
107	Aubechies	50.573856	3.676918			X	1	3
111	Ormeignies	50.596081	3.750702			X	1	3
115	Marcilly	47.762504	1.009526			X	0	0
116	Marolles	48.38722	3.034237	X		X	1	3
123	Bucy-le-Long	49.39136	3.39469			X	1	1
124	Longueil-Sainte-Marie	49.357707	2.717883	X	X	X	1	1
125	Pontpoint	49.302168	2.65404	X		X	1	2
126	Gonesse	48.986244	2.450113			X	1	2
127	Ormeignies	50.596082	3.750703			X	1	3
128	Marolles	48.38723	3.034238	X		X	1	3

Constantin et al., 2001; Jadin and Verniers, 1998; Praud et al., 2003). On the contrary, Bartonian silicite outcrops stem from the centre of the Paris Basin (Fig. 1), most likely being the source for supraregional resource and stone tool circulation. On-site presence of a combination of both artefact types, bracelets and long blades, seems to be the result of structured circulation networks (Bostyn, 1997, 1994; Bostyn and Lanchon, 2007; Plateaux, 1993).

In this paper, we focus on lithic production and particularly the circulation networks of Bartonian silicite originating from the Paris Basin. The dataset is constituted by the presence or absence of this raw material at the sites. Furthermore, the sequences of the CO identified at the sites are recorded by 4 levels (Fig. 5):

1. All or almost all (sometimes the very first flakes of shaping are missing) of the sequences of the CO are identified at the sites, which were classified as production sites of short blades.
2. Missing sequences of the CO demonstrate that the knapping process didn't entirely take place at the location. Cores in the process of

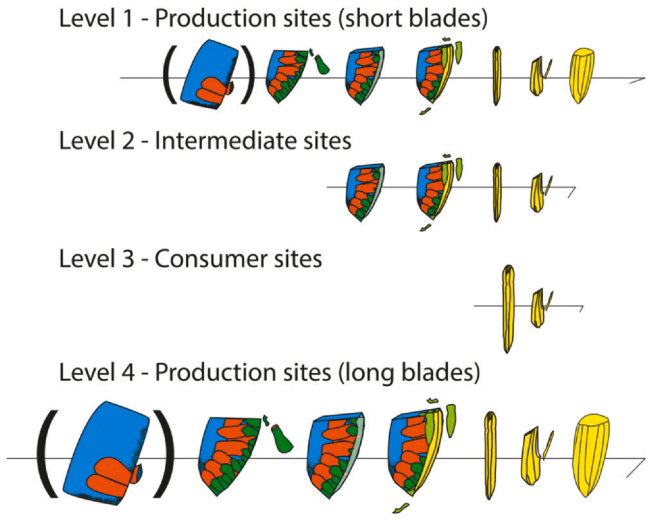

Fig. 5. Illustration of the various sequences of the CO, facilitating the classification of sites into four distinct levels. The production of long blades demanded a significantly higher level of skills compared to the production of short blades.

debitage (material residuals from production process) could have been introduced and then knapped locally. These sites are dependent on others and were classified as intermediate sites.
3. Only blades and final products were identified. Sites were classified as consumer sites.
4. Production sites with all CO present. However, particular manufacturing skills allow for the production of particularly long blades (13–20 cm), which differ from the average material. In the present stage of research, these sites are considered to be exclusively responsible for the long-distance circulation of this raw material (e.g. Bostyn, 1997).

2.3. Environmental datasets

We deployed a digital elevation model (DEM) from the United States Geological Survey (Global Multi-resolution Terrain Elevation Data 2010 (GMTED2010), https://www.usgs.gov/coastal-changes-and-impacts/gmted2010, last accessed 4th of January 2024) to set up a friction model for the production of a cost surface as a basis for movement and network models. The raster data has a spatial resolution of approximately 173 ×173 m when cropped to the study area. This resolution has been kept for the calculation of the cost surface using the *v.net.models* network generator by Benjamin Ducke (https://github.com/benducke/v.net.models, last accessed, 18th October 2023) and implemented in GRASS (see 2.4). For visualisation reasons only, we removed parts of Great Britain from the raster data. We added the major hydrologic network based on the EU-Hydro River Network Database 2006–2012 (vector) from the copernicus hub (https://land.copernicus.eu/en/products/eu-hydro/eu-hydro-river-network-database?tab=download, last accessed, 18th October 2023) for visualisation with river Strahler order number ≥ 5. The hydrologic system does not affect the network analysis because riverbeds, channels, and valleys represent preferred transportation routes deriving from a raster with medium resolution. The location of crossing major river systems, however, can not be predicted solely on topography and the modern channelization processes and river regulations further complicate the approximation to past landscape configurations.

Geological data derived from the database created by Allard (Allard, 2022). The data comes in.csv format describing sites with Bartonian silicite findings. 144 sites are represented by 135 sites with geographical coordinates. The original database was cleaned, which means all attributes with special characters were removed and only coordinates were kept. The original projection was changed to a metre-based projection in EPSG:3035 to allow for spatial manipulation. Using the *spatstat* package in R, a Kernel Density Estimation (KDE) was performed from the sites with a sigma of 2000 m and a raster resolution of 100 m. A KDE is an intensity estimation of a spatial point process, often referred to as heatmap, in which high values characterise high intensity of observations (Crema et al., 2010). The KDE was reclassified and all values < 1 were removed and all values > 1 were set to 1. Eventually, the raster was vectorized to a polygon, representing a spatial distribution of Bartonian silicite findings (see repository to this article). Additional geological data was acquired from the BRGM (Bureau de recherches géologiques et minières) as vector files (download: http://infoterre.brgm.fr/telechargements/BDCharm50/FR_vecteur.zip, after registration, available from: https://infoterre.brgm.fr/formulaire/telechargement-carte-geologique-metropolitaine-11–000-000, last accessed, 27th of April 2023). The vector has been reprojected to a metre-based coordinate system (EPSG:3035) and cropped to the study area. Using the attributes provided with the data, we queried different types of lithology or stratigraphic units as well as age specifications. Here, we focus on the dispersal of Middle Eocene units in the Paris Basin, which also cover the Bartonian silicite records. Using the code to this article, the geological information can be subset to different units, which enables the creation of individual resource models for different geological/archaeological time slices.

2.4. Resource dependency model

In the resource dependency model, we estimated the spatial distribution of the sites as a function of the geological resource dispersal. We created individual cost surfaces for each site of the samples to calculate Least Cost Paths (LCPs) between different sets of origins and destinations. LCPs are models that calculate the most efficient route between two or more locations in geographical space (Conolly and Lake, 2006) and are a common tool in urban planning, ecology and archaeology (for example, see Balbi et al., 2021; Fabrício Machado and Miranda, 2022; Fjellström et al., 2022; Howey, 2011; Verhagen and Jeneson, 2012; White and Barber, 2012). Cost surfaces were created using the package *leastcostpath* written by Joseph Lewis (Lewis, 2023a). The cost surfaces are based on the slope of the DEM and represent the cost to travel across the landscape. In this case, we chose the algorithm "Herzog" (with neighbours = 4), implemented in the package (Herzog, 2020; 2022). Other cost functions can be selected from the package and different cost models might be appropriate for reconstructing networks of different purposes (Herzog, 2022). Using the geological layer as destination and the archaeological sites as origins, we calculated LCPs between each site and the closest geological unit. However, we do not refer to euclidean distance between sites and geology but use the landscape permeability as a factor. For this reason, we load the Bartonian silicite silicitespatial data (Allard, 2022) that is provided as a related file from the repository to this article. From the point distribution of Bartonian silicite records, we perform a KDE using the *spatstat* (Baddeley et al., 2015) and the *terra* (Hijmans, 2023) package and a window of operation that is defined as the extent of the site distribution buffered with a 50 km spatial buffer. The records were turned into a *ppp*-object, which is a point pattern dataset in the two-dimensional plane (Baddeley et al., 2015). After testing multiple bandwidths, we use a bandwidth (sigma) of 2000 m and a resolution of 100 m for the intensity estimation. KDE values are reclassified so that all negative residuals as well as values < 1 were removed. A vectorized binary dataset with values ranging from 0 to 1 created a geological outcrop polygon of high probability Bartonian silicite distribution. Using the polygons as linestrings, we sampled 10000 points with a mean distance of about 120 m between each point that represent the Bartonian outcrops.

To evaluate the relationship between sites and covariate, we preprocessed the site distribution samples of the stages. We deleted duplicates before the run, which involved close neighbours that would fall

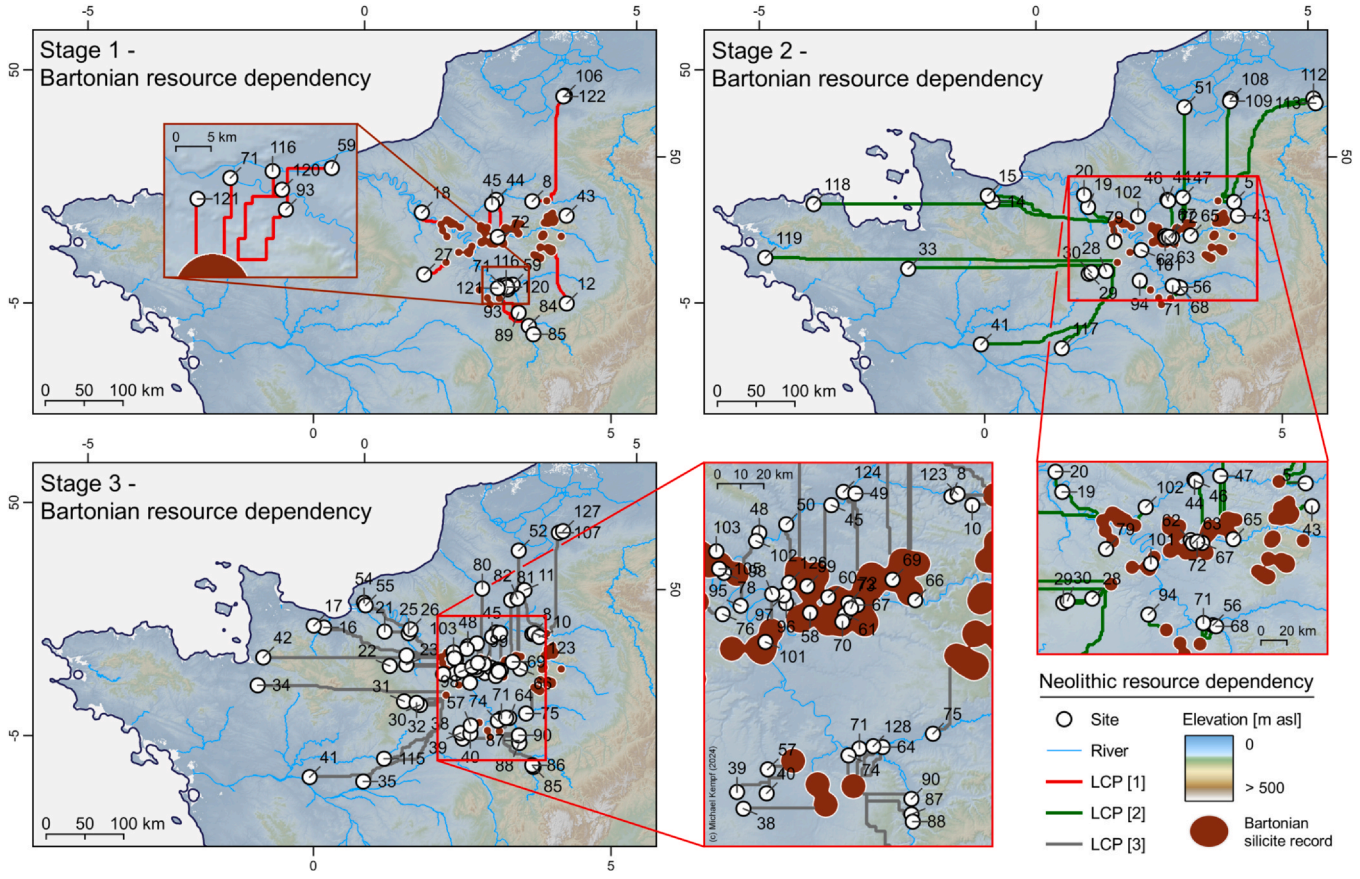

Fig. 6. Early Neolithic resource dependency models for stage 1, stage 2, and stage 3 and the Bartonian silicites based on LCP of each site compared to the best-energy-fit geological location. Major Bartonian silicites are located in the Paris Basin, according to the database of Bartonian outcrops from the Collective Research Project Matières premières du Bassin parisien (Allard, 2022). See Table 1 in the repository for site IDs.

into the same raster cell based on the resolution of the DEM, making the sample size for stage 1 n = 19, stage 2 n = 34, and stage 3 n = 69. We then split the archaeological sample to distinguish between sites that were located directly on the geological unit and sites that were located elsewhere (see Figs. 6, 7). For each of the latter, we calculated cost surfaces based on topography for the entire study area using the approach described above. For each of the 10000 sampled geology points, we extracted the raster layer value of each sample's cost surface of all three chronological stages. Eventually, we calculated which point of the sample represents the lowest cost surface value compared to each archaeological record. Using these points as destinations and the observed archaeological sites as starting points, we created the LCP of each site and its respective geological counterpart, which resulted in three chronological LCP collections (Fig. 6).

2.5. Network analysis and movement corridors

Three approaches towards network analysis, resource dependency, and modelling of landscape permeability are presented in this paper. First, we used the *v.net.models* algorithm (Ducke and Suchowska, 2022) in GRASS GIS and the default mode via the QGIS interface. We calculated a cost surface, which raster cells represent cost travelling through a set of cells and between a starting point and ideally a destination (Conolly and Lake, 2006). In this case, the cost surface is calculated from the elevation model via the GRASS GIS interface *r.cost* in QGIS. We generate individual cost surfaces for each set of archaeological stage samples, using the input data as starting points. This produces a grid with low cost (energy expenditure) closer to each site and depending on terrain roughness and high cost with increasing distance to each site and increasing terrain roughness. The elevation model acts as a friction model (Howey, 2007; Novaline Jaga et al., 1993), underlying and controlling the energy required to travel across the landscape. Building on this, the *v.net.models* algorithm creates a complete network integrating all sites into a weighted network as described in Ducke and Suchowska (2022). Eventually, we generate three different networks for the chronological stages to estimate chronologically inherent site interconnections, potential pathway and site continuity, and the relationship of the networks to environmental features and geological units.

2.6. Connectivity and probability model

The third approach is based on a Least Cost Path analysis that connects each set of sites into a so-called FETE (*from everywhere to everywhere*) approach (Bilotti et al., 2024a; Lewis, 2021; White and Barber, 2012). Using environmental covariates in spatial analysis of site distribution patterns has been widely applied in archaeological research during the past years (for example, Carrero-Pazos et al., 2019; Kempf, 2021; Kempf and Günther, 2023). This method is based on the observation of sites compared to an explanatory covariate (mostly a gridded griddeddataset) to evaluate the extent to which the site distribution pattern is a function of the respective explanatory data (Bevan and Lake, 2013; Crema et al., 2010). Multiple approaches have successfully tested topography, geology, soil units, and resource availability using point pattern analysis (PPA) (e.g., Bilotti et al., 2024b; Brandolini and Carrer, 2021; Carrero-Pazos et al., 2019; Kempf, 2021). In this paper, we created an accumulated covariate that is built on topography, landscape permeability, and geological resource availability as factors that impact the decision-making of Early Neolithic site communities. The covariate is generated by using a combined least cost

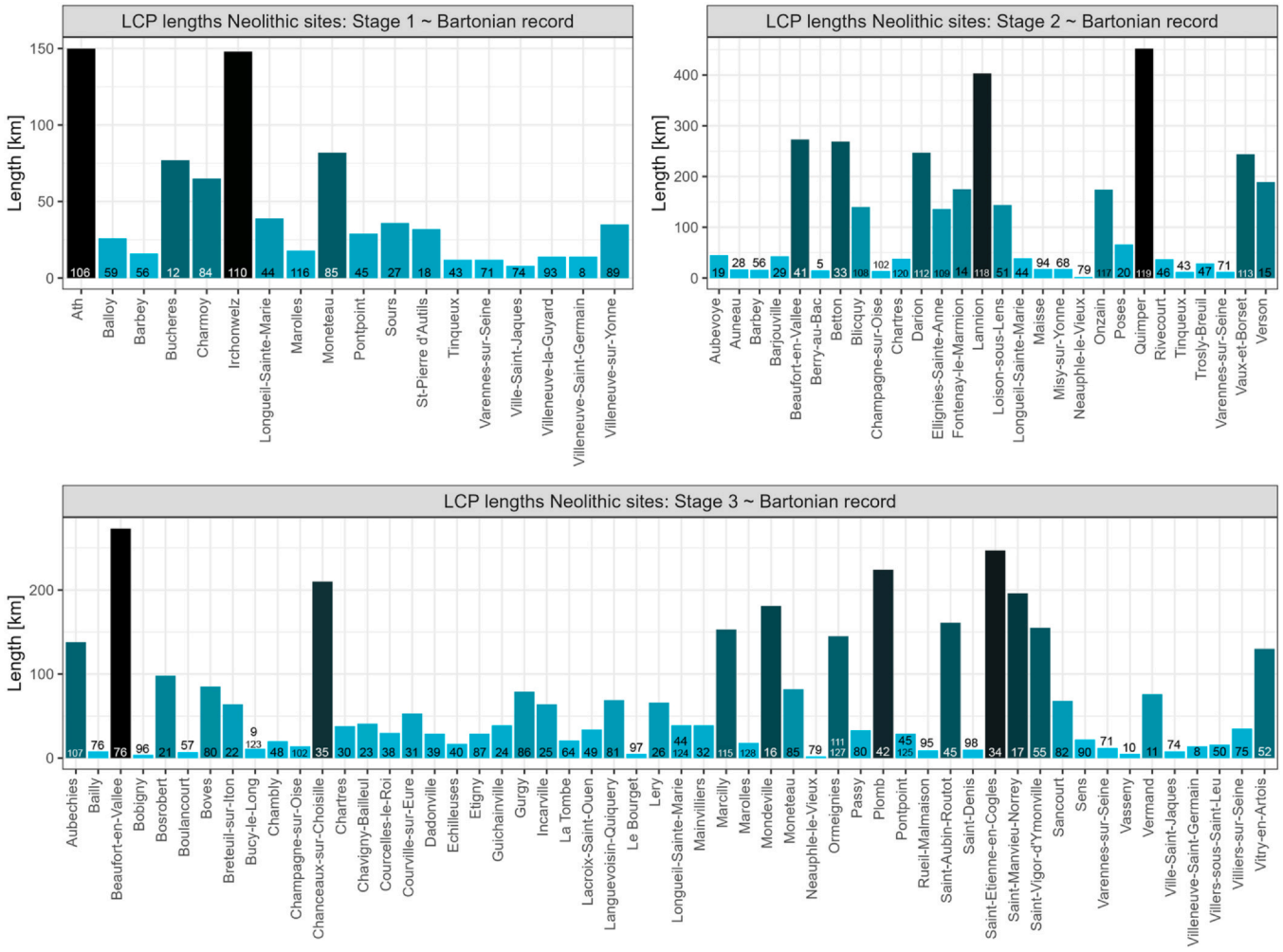

Fig. 7. Comparison of LCP lengths of all sites to the best-located available Bartonian silicite resource. Sites that fall within the record KDE do not count towards the LCP: Stage 1: Vignely; Stage 2: Rungis, Fresne-sur-Marne, Vignely, Jablines, Mareuil-Ils-Meaux, Luzancy; Stage 3: Courcelles-sur-Viosne, Jouy-le-Moutier, Maurecourt, Rungis, Gonesse, Tremblay-en-France, Claye-Souilly, Vignely, Villenoy, Mareuil-Ils-Meaux, Ocquerre, Méry-sur-Marne, Chelles, Serris, Coupvray. Duplicate location names with two individual sites and same distance (e.g., Irchonwelz) are counted only once. Site Ids are given in each bar.

approach as described above. The *leastcostpath* package (Lewis, 2023a) was used to create least cost connections from 1000 regularly sampled points along the simplified study area boundary (the landmass with a negative spatial buffer to prevent edge effects) to 1000 points sampled from the geological density estimation with a sigma of 2000 m representing the interpolated record of the Bartonian silicite. To increase computational speed and prevent memory issues, we subset to samples of 10 $\times$100 boundary points connecting with 1000 geology points and processed each subset individually. Eventually, 1 million single LCPs were merged to a single dataset and 100 million regular points were sampled from all linestrings. Using these points as input data, we created a density estimation with a sigma of 5000 m after we tested sigma of 2000, 5000, 7500, and 10000 m to detect high-intensity movement corridors across the entire study area directed towards Bartonian silicite resource distribution.

From this density estimation, we deployed the raster as an explanatory covariate against which we compared the observed archaeological sites. Using the *rhohat* function of the *spatstat* package (Baddeley et al., 2015), we calculated the underlying point process model, which we used as input variable to predict site distribution based on the empirically observed sample.

For the analysis, we convert our data into formats that are compatible with spatstat: a real-valued pixel image (*as.im* function) and a planar point pattern (*ppp*-function) (Baddeley et al., 2015). The *rhohat* function then offers a nonparametric estimate of intensity based on the covariate. Our primary objective is to ascertain the function "ρ," recognized as the resource selection function used in ecological site preference models (Baddeley et al., 2015, 2012). To achieve this goal, we construct a plot that compares the ratio estimator (referred to as "sites") with actual observed sites, incorporating a 95 % confidence interval. We assume that our point process follows a so-called *Poisson process*, which serves as a model for events occurring randomly in space or time (Grandell, 1976; Orton, 1982).

Within this plot, tickmarks are evident along the horizontal axis, with each mark corresponding to parameter values associated with observed sites. Clusters of the tickmarks characterise increased site intensity, indicative of a preference for specific ranges of covariate values. Peaks in the curve highlight locations where point concentration density is higher compared to their immediate vicinity. However, the significance of this intensity is contingent upon the associated confidence interval. A broader confidence interval implies lower confidence and may suggest the presence of isolated values or outlier clustering. Conversely, the observation of high site intensity alongside narrower confidence intervals denotes greater significance and a strong preference for specific covariate value ranges (Baddeley et al., 2015; Bilotti et al., 2024b; Kempf, 2021; Kempf and Günther, 2023).

The subsequent step entails the utilisation of the results and the covariate as input variables for a predictive model. This model aims to generate a probability map, marking areas where potential sites could be distributed based on the raster data and the empirically observed point process. To

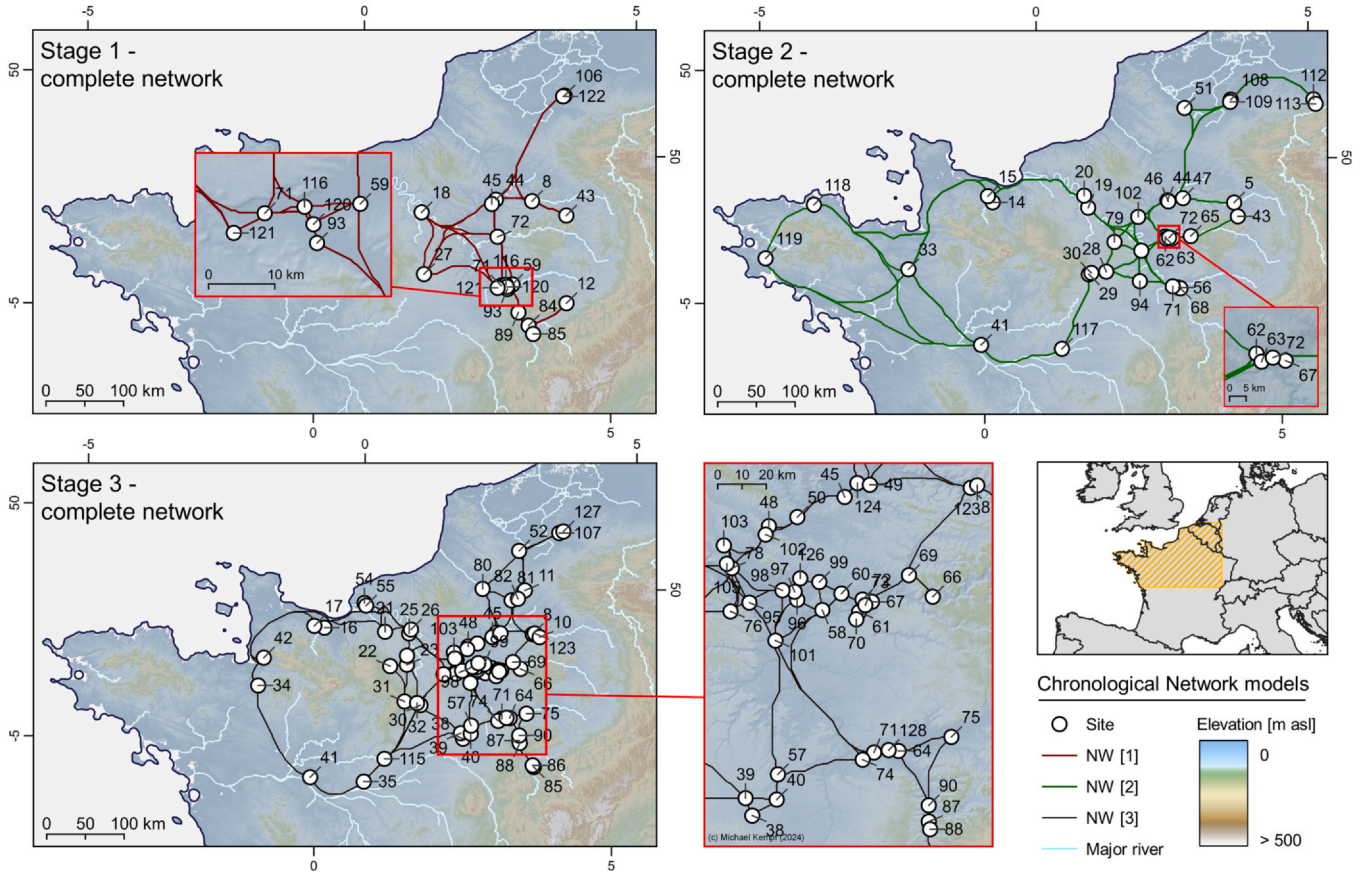

Fig. 8. Early Neolithic network models for stage 1, stage 2, and stage 3 calculated from topography using the v.net.models complete network algorithm in GRASS GIS. See Table 1 in the repository for site IDs.

create this probability map, we employ the *predict.ppm* function from the *spatstat* package. Essentially, this provides a spatial representation of the likelihood of site occurrence based on the interplay between the covariate (least cost path density) and the observed point process.

To achieve this, we used the merged sample of all archaeological sites. We can observe a high density or clustering process of sites in the Paris Basin performing a density estimation with a sigma of 20 km and a non-random spatial behaviour of site distribution compared to Bartonian silicite resources. Using the output of the point process as a covariate, we created a prediction raster from the model. However, we decided to fit the observed point process model to the calculated least cost density estimation and simulated 2000 iterations of site locations based on the provided input variables. This simulation generated 2000 sets of points (n = 230696), from which we performed a KDE with a specified sigma of 5000 m and a cell size of 250 m. To further include the areas directly affected by Bartonian silicite, we rasterized the vector, added the maximum value of the density estimation to the result and fitted it into the final covariate raster. Like this, high mobility and communication intensity is simulated across the Bartonian silicite silicitedistribution. In order to visualise regions with a high likelihood to contain containsites, we established a set of statistically derived thresholds for the density values that hold information of particularly high potential site distributions. We tested mean + SD (standard deviation); mean + 2*SD; 1st quartile (Q1), and 3rd quartile (Q3) of the data range of the KDE. We found that the extent of Q3 provides a sufficient data intensity. The density of simulated sites was cropped to the extent of Q3 and visualised with the extents of the mean + SD and mean + 2*SD.

3. Results and discussion

In the following section, we describe the three different approaches to model resource dependency and communication networks in Early Neolithic west Europe. We integrate a discussion to outline the advantage of comprehensive interdisciplinary approaches to understand environmental parameters in the decision-making process among prehistoric communities. We particularly focus on the integration of an environmental analysis into socio-cultural explanatory models and networks in Early Neolithic Europe.

3.1. Resource dependency model

The proposed resource dependency model in Fig. 6 visualises the closest location of Bartonian silicite resources compared to each single archaeological record that is not directly situated on top of the resource itself (Fig. 7). The length of the LCPs and the costs associated with travelling through the landscape varies significantly across the samples. In the early stage 1, there is only one site located within the bounds of Bartonian silicite of the Paris Basin (Vignely - id. 72) and most sites cluster around a distance of 10–25 km from the resource. Only two sites show distinct behaviour and are located up to 150 km from the closest accessible silicite sources. The stage 1 sites at Ath and Irchonwelz (id. 106, 110, 122) are somewhat dislocated and rather disconnected from the resource supply, which is visible in the network connectivity model (Fig. 9). Considering the small sample size of stage 1 sites compared to stages 2 and 3, however, outlier determination is difficult to assess. Site continuity of the Early Neolithic across all chronological stages in this area of Belgium could indicate the location of an important secondary supply or distribution centre towards northern France and into Belgium.

Stage 2 shows a completely different and heterogeneous picture with multiple sites located on and in considerable distance to the next available Bartonian silicite resource. Due to larger sample size and continuous clustering processes in the Paris Basin (see repository and

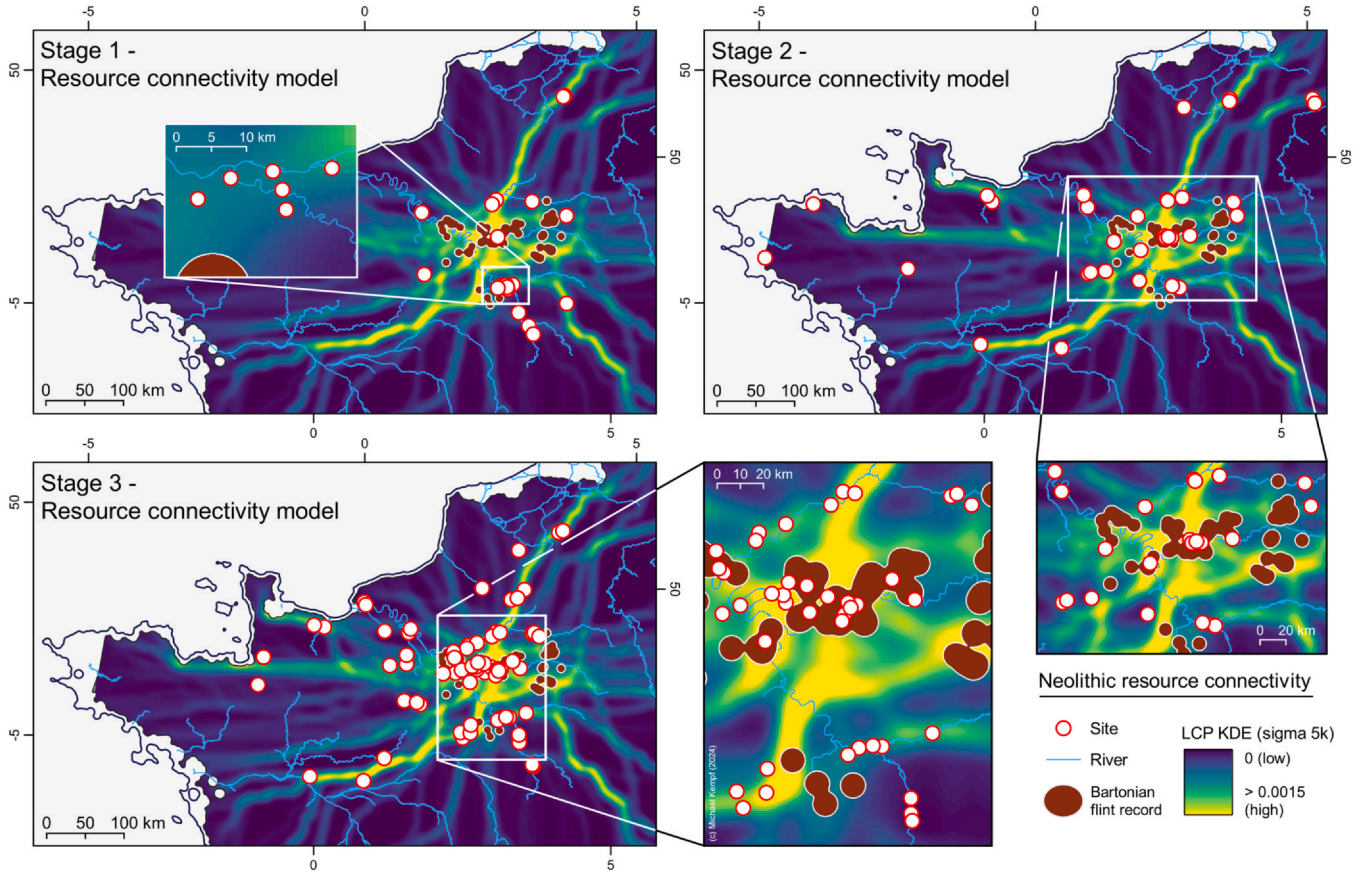

Fig. 9. RResource connectivity and probability model based on a KDE of 100 million regular points. Points were sampled from 1 million LCPs connecting the entire study area with the geological resource of Bartonian silicite located according to the database of Bartonian outcrops.

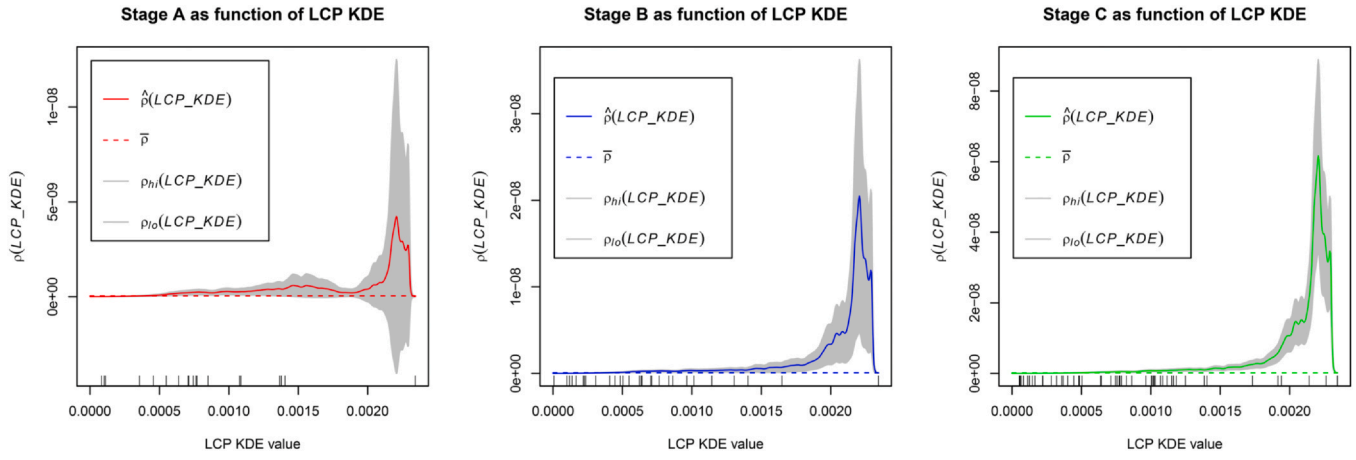

Fig. 10. Point process model of the observed archaeological sites and the simulated resource connectivity model. All sites show particular location preference towards high probability resource connectivity corridors compared to a random distribution (the dotted line) (sigma of the LCP KDE = 5000 m; KDE processed from 100 million sampled points from the LCP network).

code to this article for cluster analysis), there are more sites located with direct access to Bartonian silicite (Rungis-id. 101, Fresne-sur-Marne-id. 62, Vignely-id. 72, Jablines-id. 63, Mareuil-Iès-Meaux-id. 67, Luzancy-id. 65). This observation, however, is contrasted by the surprisingly long-distance travel with 12 sites located in over a hundred and six sites in over 200 km distance from the resource. Maximum distant sites with over 400 km from the Paris Basin are found in the western part of France.

During the later stage 3, strong clustering processes can be observed in the Paris Basin with an increasing distance relationship between resource and site location. 15 sites are situated immediately on Bartonian resource units (Courcelles-sur-Viosne-id. 103, Jouy-le-Moutier-id. 105, Maurecourt-id. 78, Rungis-id. 101, Gonesse-id. 104, 126, Tremblay-en-France-id. 99, Claye-Souilly-id. 60, Vignely-id. 72, Villenoy-id. 73, Mareuil-Iès-Meaux-id. 67, Ocquerre-id. 69, Méry-sur-Marne-id. 66, Chelles-id. 58, Serris-id. 70, Coupvray-id. 61), however, the number of sites with very close resource access increases compared to the previous chronological periods. The distance plot in Fig. 6 rather supports the hypothesis of a core distribution area located around the Bartonian resource and secondary site locations in considerable distance connected to and supplied by the circulation of products and the network.

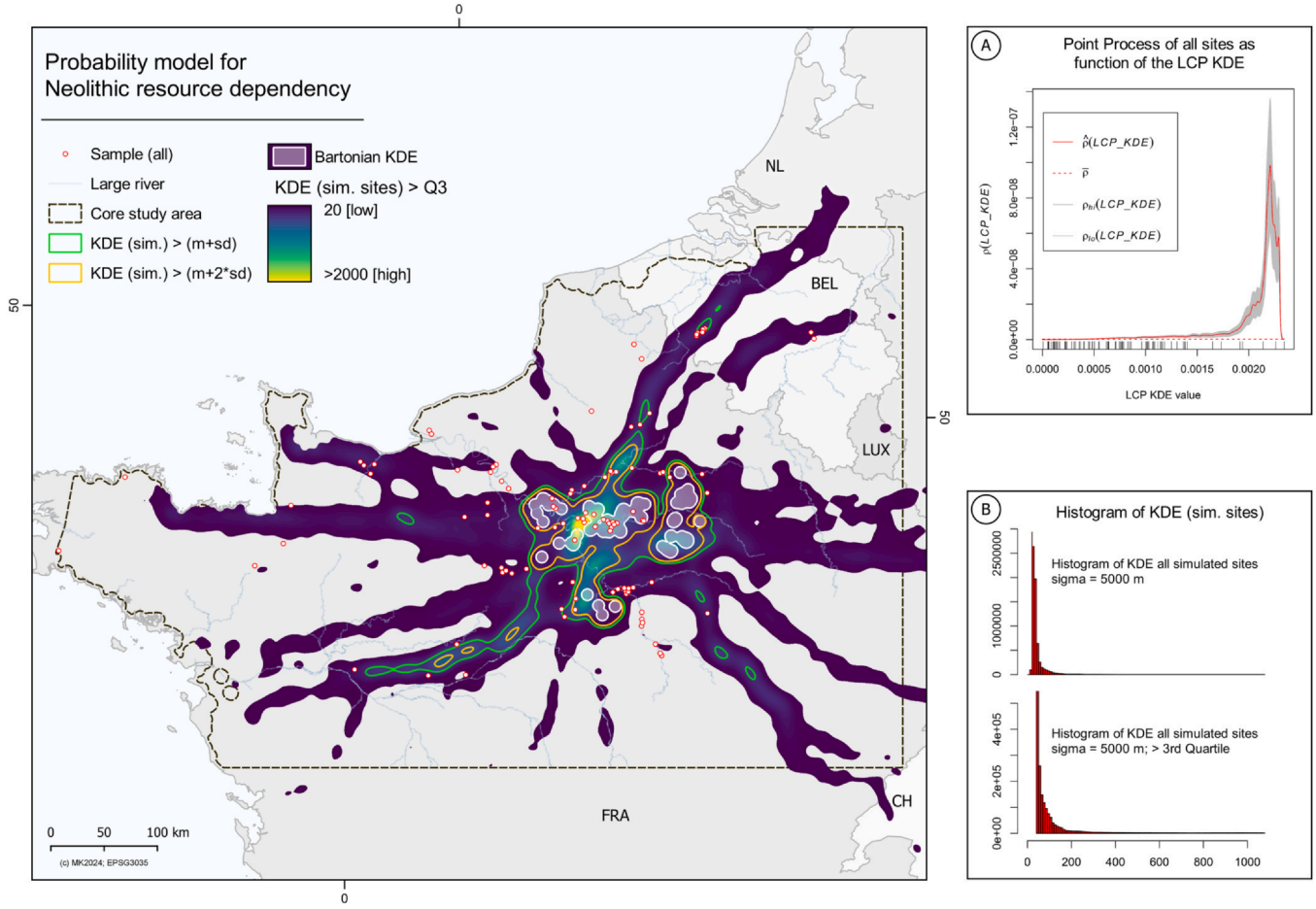

Fig. 11. Probability map from 2000 simulates sets of sites (n = 230696) based on the point process of the entire observed samples and the covariate built from the KDE of the movement corridors directed to the Bartonian silicite. The KDE was cropped using the 3rd Quartile of the range. Additional thresholds show mean + sd (green polygon) and mean + 2*sd (orange polygon). Bartonian silicite KDE is characterised as transparent-white polygon; (A) shows the point process of all sites compared to the LCP KDE; (B) shows the data range (histogram) of all cells of the KDE from simulated (predicted) sites (upper part), and all sites > the 3rd quartile of the value range (Q3 = 41).

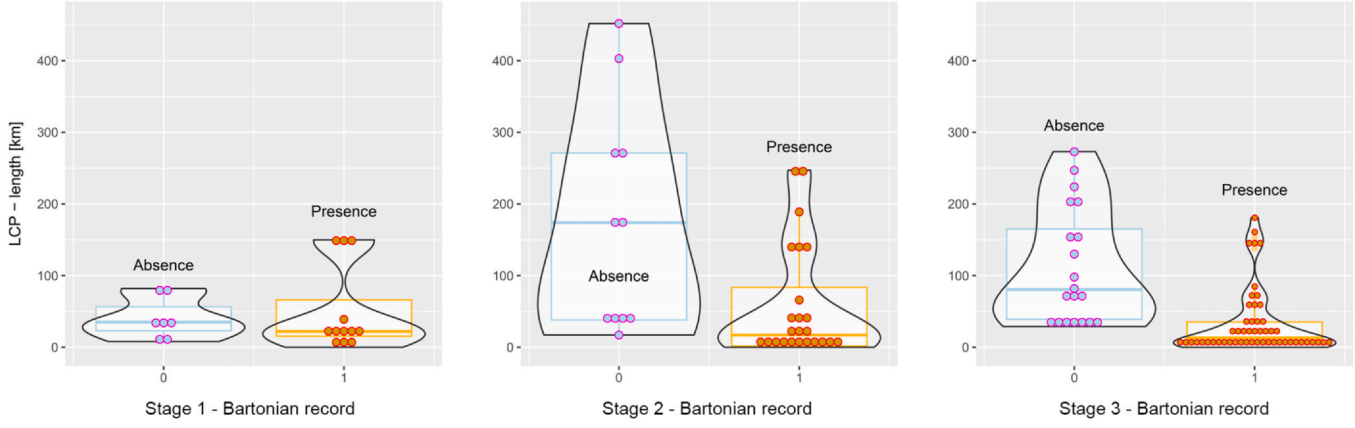

Fig. 12. Comparison of the presence/absence of Bartonian silicite on the sites and and categorised by the distance to the source.

3.2. Early Neolithic network models

Archaeological resource dependency can be visualised using a complete network analysis using the approach presented by Ducke and Suchowska (2022). Here, we distinguish three different networks with partly overlapping site locations as described in Table 1 in the repository. From the model we can observe, which sites are best located compared to the complete network and all neighbouring sites. Stage 1 shows strong linear network relationships within areas of increased clustering processes (Fig. 8). Potentially, the movement corridors are located parallel to river valleys, which are dominated by largely meandering streamflow character in the Paris Basin. Transportation and dissemination via the river, however, cannot be excluded from the hypothesis - particularly considering the low-lying areas of the plain. Towards the Morvan and the hilly margins of the Alpine foreland in the eastern part of France, communication routes would follow the terrain

Table 2
Description of the site status, based on the stages of the CO and the frequency of the sites according to the lengths of the calculated LCP at the different chronological stages (see repository for heatmaps of the LCP lengths: 10.5281/zenodo.10617484). Sites are classified following the 4 levels presented in Fig. 5 in Kempf & Denis (2024).

Stage 1	0–15 km	15–40 km	40–80 km	> 80 km
Level 1 - production center (short blades)	1	1	0	0
Level 2 - intermediate site	1	4	0	3
Level 3 - consumer site	0	1	0	0
Level 4 - production center (long blades)	0	0	0	0
Stage 2	**0–15 km**	**15–40 km**	**40–80 km**	**> 80 km**
Level 1 - production center (short blades)	5	1	0	0
Level 2 - intermediate site	2	3	0	3
Level 3 - consumer site	2	1	2	3
Level 4 - production center (long blades)	1	1	0	0
Stage 3	**0–15 km**	**15–40 km**	**40–80 km**	**> 80 km**
Level 1 - production center (short blades)	8	2	0	0
Level 2 - intermediate site	11	4	0	0
Level 3 - consumer site	6	6	5	6
Level 4 - production center (long blades)	2	0	0	0
Level 1 - production center (short blades)	**0–15 km**	**15–40 km**	**40–80 km**	**> 80 km**
Stage 1	1	1	0	0
Stage 2	5	1	0	0
Stage 3	8	2	0	0
Level 2 - intermediate site	**0–15 km**	**15–40 km**	**40–80 km**	**> 80 km**
Stage 1	1	4	0	3
Stage 2	2	3	0	3
Stage 3	11	4	0	0
Level 3 - consumer site	**0–15 km**	**15–40 km**	**40–80 km**	**> 80 km**
Stage 1	0	1	0	0
Stage 2	2	1	2	3
Stage 3	6	6	5	6
Level 4 - production center (long blades)	**0–15 km**	**15–40 km**	**40–80 km**	**> 80 km**
Stage 1	0	0	0	0
Stage 2	1	1	0	0
Stage 3	2	0	0	0

permeability with increased density of transportation routes along valleys (Fig. 9).

During stage 2, the network widens due to larger geographical spread of the sample and the integration of distant sites across the study area. Here, the slightly elevated areas of Brittany and Normandy force the network to split into two major communication routes that run along the northern coastline and via the Loire river valley to the south. Both routes join the Paris Basin cluster. In the north-eastern part of France and Belgium, the Ardennes mountain range predominates the network of the spatially remote sites.

During the final stage 3, the shift towards more focused or concentrated site dispersal is also mirrored in the dense network across clustering sites in the centre of the Paris Basin. Very clearly, the riverine networks prevail, with high traffic density across the river Seine tributaries. Most likely, a location factor of flood secure settlement spots and close access to fresh water can be considered decisive during the Early Neolithic period (e.g. Ilett, 2010). Other sites that are not directly connected to the hotspots are attached via larger network nodes comparable to the previous stage 2. The north-south differentiation is still visible in the communication corridors of stage 3 with the Loire river valley sites representing a rather detached location pattern. The hilly topography of Brittany acts as a topographic barrier for direct network connections, however, communication and transportation across the region cannot be ruled out. The bias by current archaeological knowledge can create high local uncertainties.

The network analysis approach we chose in this paper is a complete network based on an algorithm implemented in GRASS GIS. There are, however, other LCP or network approaches, building on different movement algorithms, for example Tobler or Herzog and integrated into R software as recently proposed by Joseph Lewis (Herzog, 2022; Lewis, 2023b, 2021). Much of the accuracy depends on the chosen resolution of the underlying explanatory rasters that serve as cost surface for the LCP analysis.

3.3. Resource connectivity and probability model

Depending on the resource location of Bartonian silicite, a resource connectivity and probability model has been carried out using intensity analysis from least cost paths across the study area (Fig. 9). For this reason, we deployed 1 million LCPs that connect each point on a grid across the raster with all other points representing the geological outcrops in the Paris Basin. Eventually, a density estimation of points sampled from these lines show the most probable movement corridors when travelling from a random location to the next geological resource. From this density, we can identify hotspots of dissemination corridors, for example reaching towards the Loire river valley to the south-west or towards Belgium, connecting far reaching sites to the clustered centre of the Early Neolithic in France. Particularly striking is the integration of Belgian sites in the north-east or remote sites to the south and the far west, respectively. If not connected via river valleys, for example the river Seine tributaries to the south, the sites are linked to the resource clusters via high probability movement corridors. Eventually, this points strongly into the direction of topographical features being decisive for the distribution of sites and the overall connection to resource networks.

To estimate the influence of the connectivity and probability model, a point process model has been established using the *spatstat* package. It estimates if the distribution of the total number of sites is a function of the covariate. However, the significance of this intensity relies on the confidence interval, displayed as a grey envelope in the plots (Fig. 10). Fig. 10 shows the site distribution on the x-axis representing the covariate parameter value linked to observed sites. Clustering of these sites show areas with an increased site concentration and a small confidence interval suggests a preference for specific ranges of covariate values. TThe geological density estimation has been added to the covariate as maximum value to simulate high movement and interaction directly connected with the location of the resource. Hence, this assigns all sites located within the resource location a high connectivity value.

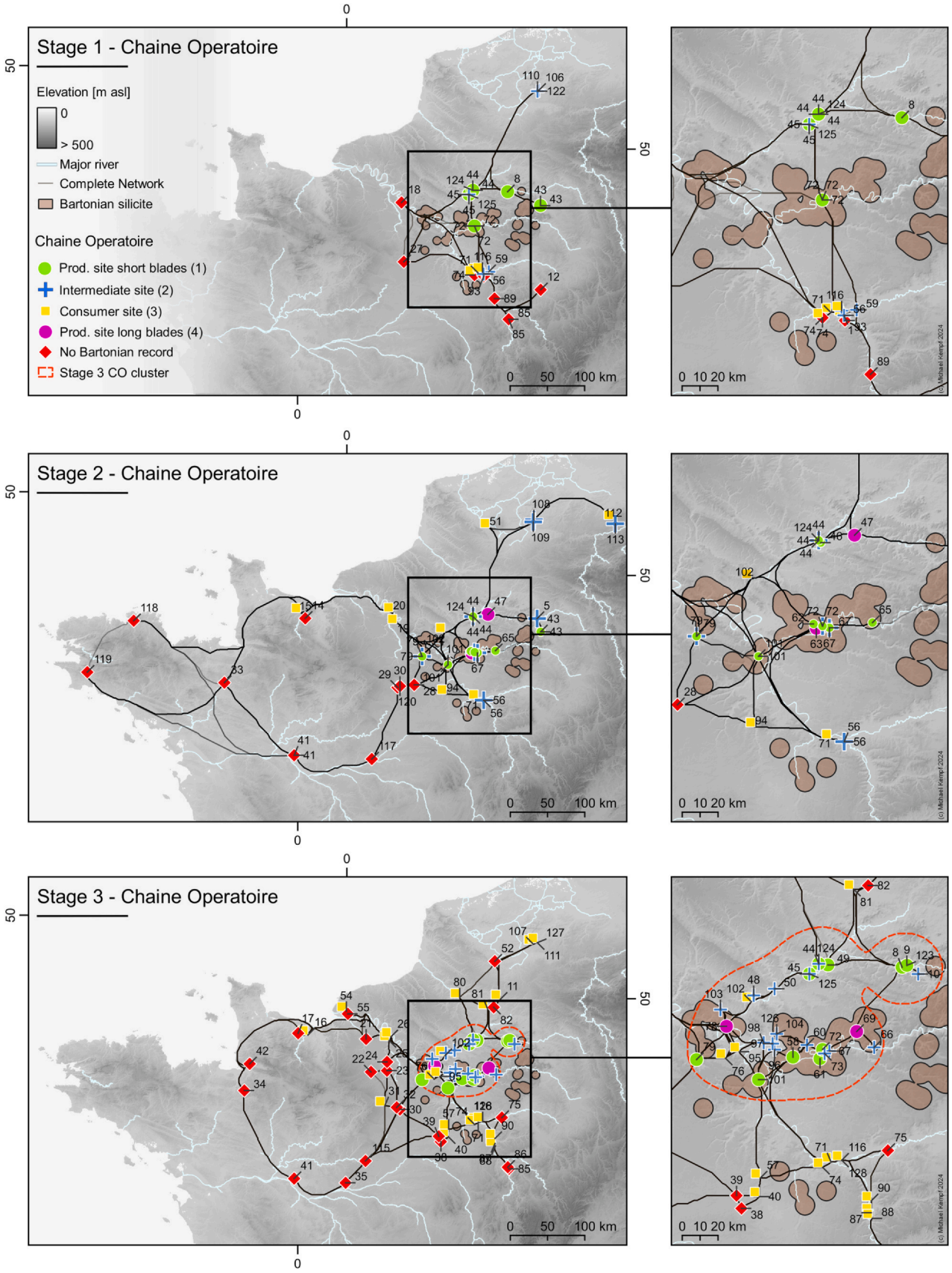

Fig. 13. Panel map illustrating the distribution of sites according to the CO of Bartonian blade production during the three stages. Outside the central sites cluster of stage 3 (highlighted by the red dashed line), only blades (either semi-finished or finished products) were circulated. The concentration of intermediate sites within the clustered area implies limited access to the sources and a potential control of the initial supply chain by the production sites. See Table 1 in the repository for site IDs.

We can observe site preferences for high covariate values throughout all stages. Stage 1, represented by a smaller sample size, shows non-random site distribution with preference of intermediate and higher values (> 0.0005). At very high values, the distribution gets less significant with a larger confidence interval. Stage 2 shows stronger clustering at values between 0 and over 0.001 with few sites located at higher values. However, there is a stronger site observation at middle range values deriving from the increasingly clustered site dispersal across the Paris Basin. Low value outliers are connected to the wide range of geographical origin of the sites, now dispersed across the entire study area. Stage 3 now shows strong preference for mid-range and high values, which is connected to the strong clustering process in close distance and directly on the resources as well as the connected sites located rather remotely.

Finally, we can use the point process model (PPM) from the entire sample to produce a probability model based on the PPM and the covariate (Fig. 11). The result of the probability model is cropped to the extent of the 3rd quartile of the data range and visualised as a continuous raster with low values indicating low site probability and high values showing high probability. Further thresholds are provided as the mean plus the standard deviation (m + sd) and the mean plus twice the standard deviation (m + 2*sd) to compare different probability ranges across the simulation. Note that for the PPM underlying the predictive model, the polygons of the Bartonian silicite outcrops were added to the raster covariate as equal maximum values of the KDE. This produces additional high values in areas that are covered by the resource itself and simulates high movement probability and strong resource-communication interaction where the geological resource is strongly abundant.

From the model, we observe a strong site probability in the centre of the Paris Basin with secondary centres east to the basin and along the well-connected communication corridors towards the Loire river and to the northern parts, including Belgium. Hence, site probability is not only controlled by the spread of the silicite resource only, but equally builds on the topographic conditions and the accessibility and permeability of the landscape. Remotely located sites could simply be supplied with raw material via well-connected transportation corridors and a well-developed redistribution system of raw material based on intermediate and consumer sites. A few sites are located outside of the high probability corridors. This can be due to the 3rd quartile threshold that we applied to the density estimation of the simulated points. These sites, however, are connected via the network as displayed in Fig. 8. Furthermore, the density estimation shows a strong central dependency for the Paris Basin, which is caused by high site density and second-order properties of the point pattern. In this context, second-order properties refer to spatial interaction and feedback within the point pattern itself, creating interdependencies among closely connected sites or, in other words, site locations depend on the locations of other sites. As an effect, the density of sites in the central Paris Basin cluster is a function of this spatial interaction, which gives the impression of outlier or site exclusion of more remote sites. Using an interplay of the network model and its spatial feedback, we can draw conclusions about the integration of distant sites compared to clustered site behaviour of the central distribution area.

3.4. Early Neolithic site networks as social and environmental constructions

Comparison between the LCP with the presence or absence of Bartonian silicite at the different sites demonstrates an important differentiation between the samples (Fig. 12 and Table 2 in the repository to this article). During stage 1, supply of Bartonian silicite took place independently of the distance to the source. Some sites close to the outcrops did not yield any Bartonian silicite (e.g. sites ids. 18, 27, 74, 89 and 93), while others, particularly the three sites in Belgium (ids. 106, 110, 122), are located far from the outcrops (around 150 km). Stage 2 yields an extension of the occupation area beyond the Paris Basin, as recorded by settlements located over 450 km in distance to the resource. This extension of activity spheres and networks, however, had little impact on the overall distribution of Bartonian silicite and the mean distance to the resource is mostly comparable across the 3 stages. On the other hand, the distribution of Bartonian silicite follows a preferential north-eastern direction. For example, sites located around Chartres (ids. 28, 29, 30 and 120, LCP < 45 km) are completely excluded from the circulation network even though they are located closer to the sources than the sites from northern France (id. 51, LCP = 144 km) or Belgium (ids. 113, 112, respectively 244 and 247 km). All the sites originating from the western part of the study area are excluded from the supply chain. During stage 3, the areas where sites provided Bartonian silicite seem to be reduced with a maximum distance of 181 km in Mondeville (id. 16) and 161 km in Saint-Aubin-Routot (id. 54). The north-eastern preference of the circulation ended around that time, as has been previously suggested by Bostyn et al. (2019). The distribution of Bartonian silicite is more related to the source's distance.

During stage 1, no long blade production sites (level 4) have been identified so far. The site of Tinqueux “la Haubette” (id. 43) could be a turning point with a few indications for the production of longer blades (Hachem et al., 2021). Most likely, the circulation started from the production sites (n = 2, id. 43 and Pontpoint- id. 45) and was directed towards all other sites. According to the network model (Fig. 8), both routes could have been used to arrive at the three Belgian sites (ids. 106, 110, 122), located quite considerably from the resource outcrops. The raw material at those sites testifies that the knapping process occurred on-site (Table 2 in the repository to this article). It has previously been suggested that these could be the result of mobile knapping specialists originating from the Paris Basin (Denis, 2019). The site of Vignely (id. 72) where the start of the CO is missing, could, according to the model, rather be related to the production site id. 45 than to the site id. 43. It could be an intermediate location toward the Seine-Yonne confluence cluster (ids. 1, 56, 59, 71, 74, 93, 116). Three sites are, however, lacking the initial start of the CO and only one site provided blades (consumer site, level 3, id. 1). This is the only case observed in the entire stage 1. All these sites are located close to potential silicite resources, in approximately 16–26 km distance according to the least cost path model. Here, the distance to the resource is considerably shorter compared to the production site (level 1) id. 45 in the Oise valley (29 km). We hypothesise the possibility of an autonomous cluster where the spatial segmentation of the CO took place. The start of the CO could have occurred at the outcrops and only pre-formed cores could have been transported to the sites. Redistribution of blades happened frequently towards consumer sites. This could also be supported by the fact that in this area and during the entire chronology, Bartonian blades were rather short compared to the products from the very centre of the Paris Basin (Augereau, 2004; Denis, 2012). Augereau (2004), for example, has proposed knapping specialists that engage in the production and redistribution of blades, particularly focusing on the best available local raw materials.

During Stage 2, two significant long-blade production sites (level 4), Trosly-Breuil (id. 47) in the Aisne Valley and Jablines (id. 63) in the Marne Valley, are identified (Bostyn, 1997, 1994). As illustrated in the model (Fig. 8), Trosly-Breuil emerges as the primary supplier along the preferential north-eastern road leading to northern France and Belgium. The CO shows that both sites in western Belgium (Blicquy-id. 108 and Ellignies-Sainte-Anne id. 109) played a crucial role in redistributing cores and blades towards more distant locations, such as Vaux-et-Borset (id. 113). Additionally, this redistribution likely extended to providing blades to the communities of Darion (id. 112) (Denis, 2019) as demonstrated also by the model. Our findings support the hypothesis that these intermediate sites (level 2, ids. 108 and 109), located at distances of 136 and 140 km to the outcrops, could have functioned as pivotal secondary supply hubs towards northern France (Loison-sous-Lens, id. 51. This observation reinforces the coherence of

our model and underscores the significance of these intermediate sites (level 2) in the broader regional network of long-blade production and distribution during this stage. An additional significant circulation route emerged, extending towards Normandy along the Seine Valley. Both Jablines and Trosly-Breuil are likely to be to be the origins of this movement corridor. According to the network model, both pathways would share analogous redistribution structures. This involves passing through a central production centre for small blades (level 1), such as Longueil-Sainte-Marie (id. 44) for the northern route and Rungis (id. 101) or Fresne-sur-Marne (id. 62) for the eastern route, followed by an intermediate site (level 2) at Rivecourt (id. 46) or Neauphle (id. 79). On the northern path, Champagne-sur-Oise (id. 102) would serve as the initial consumer site (level 3). Eventually, this would support the *down-the-line model of redistribution* proposed by Colin Renfrew (1984). This model posits a sequential transfer of artefacts through production centres to consumer sites with a decreased number of artefacts with increasing distance. Looking closer at the western part of the model, Neauphle, Rungis, and Maisse (id. 94) appear to not function as intermediates to facilitate towards the site clusters surrounding Chartres (ids. 28, 29, 30, 120), which are a bridge towards the Loire river and the southern corridor. But Neauphle and Rungis may have played a major role in the redistribution of artefacts directed towards Normandy, highlighting their significance to the north-western path. In contrast, Maisse is identified as a consumer site (level 3) situated near the autonomous cluster at the Seine-Yonne confluence in the south-eastern part of the Paris Basin (ids. 56, 68, 71), where no long-blade production sites have been identified. We propose the hypothesis that Bartonian silicite in this area may lack the distinctive identity markers that characterise other regions. The absence of artefact circulation along this southern route could be attributed to the strong affiliation of these sites with the Seine-Yonne area (ids. 56, 68, 71). This proposition gains support from the potential resource connectivity model (Fig. 9), which indicates that the highest values are concentrated in this geographical area. The isolation of the south-eastern area of the BVSG occupation is further evident in the probability model for resource dependency (Fig. 10), whereas its connection to the Loire valley region appears to be less significant. Stage 3 shows a notable reconfiguration in the organisation of the circulation network. Strikingly, all sites located beyond the densely interconnected cluster at the heart of the Paris Basin only delivered blades (Fig. 13).

The introduction of two novel long-blade production centres, Ocquerre (id. 69) and Maurecourt (id. 78), made a significant technological development due to their capacity to supply in all directions, according to the network model (see Fig. 8). However, Maurecourt emerged as the most likely supplier for the Normandy corridor. An observable trend is the increasing presence of intermediate sites (level 3) within the central region of the Paris Basin (Table 2, see repository). These intermediate sites are characterised by the introduction of preformed blocks, even though they are located at equivalent distances from the deposits. Unlike the producer sites, which cover the entire CO (raw blocks) and therefore indicate direct access to the source, this access could probably be limited or indirectly indicate level 3 sites. This shift suggests an increased interdependence among sites within the area, likely indicative of increased resource control by the production centres. The simultaneous decline of local production in the Seine-Yonne cluster might have been linked to the same transformative dynamics during Stage 3. The transformation in the organisation of the circulation network highlights the complex relationships between sites situated directly or in close proximity to the resources. It suggests a probable reinforcement of control over these sources, that enabled the establishment of long-distance connections in multiple directions. This is in line with the observations highlighted by the point process model of the observed archaeological sites and the simulated resource connectivity model (Fig. 9).

The analysis of the circulation of Bartonian silicite, based on the spatial segmentation of the blade production CO contributes to a better understanding of the socio-cultural dynamics in the BVSG. Considering the variability observed among the three stages, the rapid cultural evolution can be summarised as follows:

Stage 1: Sites are predominantly concentrated in the south-eastern region of the Paris Basin, particularly around the Seine-Yonne area. In general, sites are situated around 10–25 km from the Bartonian silicite outcrops in the central Paris Basin. No long-blade production sites have been identified so far. However, evidence for long-distance circulation networks have been proposed, with a prevailing direction towards the Belgian sites and suggesting the mobility of specialised craftsmen. We propose that the Seine-Yonne cluster area may function independently in terms of both the production and distribution of the raw material. The Seine river appears to function as a boundary in the circulation of Bartonian silicite. These distinct territorial dynamics may be reflected in the entire production system as previously pointed out elsewhere (Augereau, 2004; Bostyn, 1994).

Stage 2: Two key phenomena characterise Stage 2. There is a significant expansion of the BVSG occupation area, with sites extending beyond 400 km from the centre of the Paris Basin, where a cluster of sites has been identified. Simultaneously, specialised sites emerged that focused on the production of long blades with a topographic preference for valley situations. The circulation of Bartonian silicite extends approximately 250 km to the North-East, highlighting the development of a redistribution center in western Belgium. In contrast to this, long blade records now extend to the Seine Valley, particularly in the direction towards Normandy. However, the western peripheries remain excluded from this circulation network, with a significant barrier along the southern route leading to the Loire valley. During this period, circulation patterns were influenced by a strong interdependence among the sites, which are integral components of redistribution chains.

Stage 3: The resource connectivity and probability model now reveals a pronounced clustering process in close proximity to and directly on top of the resources in the centre of the Paris Basin - contrasting the well-connected sites located at greater distance. The organisation of the production and circulation exhibits a distinct and unique pattern compared to the previous stages. Two new production centres for long blades emerged, forming a west-east territorial differentiation. Particularly noteworthy is the significant increase in the number of intermediate sites in the same area that are located in close proximity or directly on the resources. This probably indicates the absence of direct access to the resource for all the other communities. The interdependence between these sites and the production centres shows the development of a much more organised control over the resources in this particular region. Only blades circulate beyond these clusters. This shift not only emphasises the evolving dynamics within the network but also highlights the strategic importance of resource control in facilitating extensive connectivity across the archaeological landscape.

4. Conclusion

This paper investigates the circulation networks of identity markers for the early Neolithic period in France and Belgium based on Bartonian silicite for high quality stone tool production. The distribution of silicite played a major role to establish long and short distance networks, partly based on environmental components as driving factors of pathway continuities. The model we present integrates both, an environmental analysis to trace these networks as a function of underlying covariates and a social explanatory factor of supply chains that emerged from the distance relationship of the central raw material distribution and the scattered Early Neolithic sites across the study area. Our focus is exclusively on silicite resource dispersal, however, other raw materials provided similarly important networks, for example, schist bracelets that served as a complementary component to this circulation (Plateaux, 1990; Pétrequin). We present an interdisciplinary research approach, combining quantitative models based on accumulative cost functions, chronologically differentiated network models, and a

probability model for site distributions using a point process model, along with an archaeological analysis and the concept of the Chaine Operatoire. This integrative model provides valuable insights into resource dependency and communication networks in early Neolithic western Europe. The three chronological stages underlying this study reveal distinct patterns and highlight the evolving dynamics of social and cultural occupation during that period. Furthermore, the results strengthen the mutual benefits of complementary approaches in archaeology, with a particular focus on how archaeological data analysis and interpretation can help to sharpen quantitative explanatory and exploratory models and vice versa. In forthcoming analyses, the model can further be utilised to test the hypothesis using a variety of raw materials and by incorporating additional CO data. Other exchange networks can be included in the models as this period coincides with the beginning of the long distance circulation networks of polished axes produced from Alpine resources (Pétrequin et al., 2006). The patterns of resource dispersal and site distribution identified by our model offer a comprehensive perspective on Early Neolithic social dynamics, emphasising the intricate relationships between resource management, settlement patterns, and communication networks in the archaeological landscape of western Europe.

Author statement

The authors declare no conflict of interest.

CRediT authorship contribution statement

Michael Kempf: Writing – review & editing, Writing – original draft, Visualization, Validation, Supervision, Software, Resources, Project administration, Methodology, Investigation, Funding acquisition, Formal analysis, Data curation, Conceptualization. **Solène Denis:** Writing – review & editing, Writing – original draft, Validation, Supervision, Resources, Project administration, Methodology, Investigation, Funding acquisition, Formal analysis, Data curation, Conceptualization.

Declaration of Competing Interest

The authors declare that they have no known competing financial interests or personal relationships that could have appeared to influence the work reported in this paper.

Acknowledgments

The authors are particularly grateful for the constructive suggestions of two anonymous reviewers and the editorial comments received from Jan Kolář. MK's research project at Basel is funded by the Swiss National Science Foundation (SNSF/SNF): Project EXOCHAINS - Exploring Holocene Climate Change and Human Innovations across Eurasia (SNSF grant number: TMPFP2_217358).

Supporting information

To replicate the results, we uploaded an experimental code and data to follow the workflow: https://zenodo.org/records/10617484

Table 1 with site distribution data and locations as well as Table 2 with network information can be accessed via this repository: https://zenodo.org/records/11165502

References

Allard, P., 2022. Matières premières du Bassin parisien: les silex cénozoïques d'Ile-de-France (Rapport triennal 2019-2022, Projet Collectif de Recherches). DRAC Île-de-France, Ministère de la Culture, Paris.

Allard, P., Bostyn, F., 2006. Genèse et évolution des industries lithiques danubiennes du Bassin parisien, in: Contribution Des Matériaux Lithiques Dans La Chronologie Du Néolithique Ancien et Moyen En France et Dans Les Régions Limitrophes. Session de l'EAA (Lyon, septembre 2004), Oxford, Archaeopress (BAR International Series), p. 28-52.

Augereau, A., 2004. L'industrie du silex du Ve au IVe millénaire avant J.-C. dans le sud-est du Bassin parisien, Documents d'Archéologie française. Maison des Sciences de l'Homme, Paris.

Baddeley, A.J., Chang, Y.-M., Song, Y., Turner, R., 2012. Nonparametric estimation of the dependence of a spatial point process on spatial covariates. Stat. Its Interface 5, 221–236.

Baddeley, A., Rubak, E., Turner, R., 2015. Spatial Point Patterns: Methodology and Applications with R. Chapman and Hall/CRC Press, London. https://doi.org/10.1201/b19708

Balbi, M., Croci, S., Petit, E.J., Butet, A., Georges, R., Madec, L., Caudal, J., Ernoult, A., 2021. Least-cost path analysis for urban greenways planning: a test with moths and birds across two habitats and two cities. J. Appl. Ecol. 58, 632–643. https://doi.org/10.1111/1365-2664.13800

Bedault, L., Hachem, L. 2008. Recherches sur les sociétés du Néolithique danubien à partir du Bassin parisien: approches structurelles des données archéozoologiques, in: Fin Des Traditions Danubiennes Dans Le Néolithique Du Bassin Parisien (5100-4700 Av. J.-C). Autour des Recherches de Claude Constantin, Mémoires de La SPF. Société préhistorique française et Presses Universitaires de Namur, Paris, Namur, pp. 221-244.

Bevan, A., Lake, M., 2013. Intensities, interactions and uncertainties: some new approaches to archaeological distributions. In: Bevan, A., Lake, M. (Eds.), Computational Approaches to Archaeological Spaces. Left Coast Press, Walnut Creek, California, Walnut Creek, California, pp. 23.

Bilotti, G., Kempf, M., Leon, J.M.M., 2024a. Modelling land and water based movement corridors in the Western Mediterranean: a Least Cost Path analysis from Chalcolithic and Early Bronze Age ivory records. Archaeol. Anthropol. Sci. https://doi.org/10.21203/rs.3.rs-3410688/v1

Bilotti, G., Kempf, M., Oksanen, E., Scholtus, L., Nakoinz, O., 2024b. Point Pattern Analysis (PPA) as a tool for reproducible archaeological site distribution analyses and location processes in early iron age south-west Germany. PLoS ONE 19 (3), e0297931. https://doi.org/10.1371/journal.pone.0297931

Bonnardin, S., 2009. La parure funéraire du Néolithique ancien en bassins parisien et rhénan. Matériaux, techniques, fonctions et usage social, Mémoire XLIX, Société préhistorique française, Paris.

Bostyn, F., 1994. Caractérisation des productions et de la diffusion des industries lithiques du groupe néolithique du Villeneuve-Saint-Germain (Thèse de doctorat). Paris X, Nanterre.

Bostyn, F., 1997. Characterization of Flint Production and Distribution of the Tabular Bartonian Flint during the Early Neolithic (Villeneuve-Saint-Germain Period) in France. In: Schild, R., Sulgostowska, Z. (Eds.), Man and Flint. Presented at the 7e International Flint Symposium, Institute of Archaeology and Ethnology. Polish Academy of Sciences, Varsovie, pp. 171–183.

Bostyn, F., 2008. Les importations en silex bartonien du Bassin parisien sur les sites blicquiens en Hainaut belge, in: Fin Des Traditions Danubiennes Dans Le Néolithique Du Bassin Parisien (5100-4700 Av. J.-C). Autour Des Recherches de Claude Constantin, Mémoires de La SPF. Société préhistorique française et Presses Universitaires de Namur, Paris, Namur, pp. 397–412.

Bostyn, F. (dir), André, M.-F., Beurion, C., Billard, C., Hachem, L., Hamon, C., Lanchon, Y., Munaut A.-V., Praud, I., Reckinger, F., Ropars, A., 2003. Néolithique ancien en Haute-Normandie: le village Villeneuve-Saint-Germain de Poses « sur La Mare » et les sites de la boucle du Vaudreuil. Mémoires et Travaux de La Société Préhistorique Française, 4, Paris.

Bostyn, F., Charraud, F., Denis, S., 2019. Variabilités techniques, évolutions et aires d'influence des centres de productions laminaires au sein de la culture de Blicquy/ Villeneuve-Saint-Germain, in: Préhistoire de l'Europe Du Nord-Ouest: Mobilité, Climats et Identités Culturelles. 28e Congrès Préhistorique de France, Congrès Préhistorique de France. Société préhistorique française, Amiens, pp. 43–56.

Bostyn, F., Lanchon, Y., 2007. Sériation chronologique et analyse spatiale dans la culture de Villeneuve-Saint-Germain: les exemples du village de Poses (Eure) et de la basse vallée de la Marne, in: Brun-Ricalens, F.L., Valotteau, F., Hauzeur, A. (Eds.), Relations interrégionales au Néolithique entre Bassin parisien et Bassin rhénan, Archaeologia Mosellana. Musée National d'Histoire et d'Art du Luxembourg, pp. 209–228.

Brandolini, F., Carrer, F., 2021. *Terra, Silva et Paludes*. Assessing the role of alluvial geomorphology for late-holocene settlement strategies (Po Plain – N Italy) through point pattern analysis. Environ. Archaeol. 26, 511–525. https://doi.org/10.1080/14614103.2020.1740866

Burnez-Lanotte, L., Caspar, J.-P., Vanguestaine, M., 2005. Technologie des anneaux en schiste dans le groupe de Blicquy/ Villeneuve-Saint-Germain à Vaux-et-Borset (Hesbaye, Belgique): interférences de sous-systèmes techniques. Bull. De. la Soci. été Pr. éHist. Française 102, 551–596.

Carrero-Pazos, M., Bevan, A., Lake, M.W., 2019. The spatial structure of Galician megalithic landscapes (NW iberia): a case study from the Monte Penide region. J. Archaeol. Sci. 108, 104968. https://doi.org/10.1016/j.jas.2019.05.004

Conolly, J., Lake, M., 2006. Geographical information systems in archaeology. Cambridge Manuals in Archaeology. Cambridge University Press, Cambridge. https://doi.org/10.1017/CBO9780511807459

Constantin, C., 1985. Fin du Rubané, céramique du Limbourg et Post-Rubané en Hainaut et en Bassin Parisien. BAR International serie. BAR Publishing, Oxford.

Constantin, C., Hance, L., Vachard, D., 2001. Un réseau d'échange de calcaire utilisé pour la fabrication d'anneaux pendant le groupe de Villeneuve-Saint-Germain. Bull. De. la Soci. été Pr. éHist. française 98, 245–253.

Crema, E.R., Bevan, A., Lake, M.W., 2010. A probabilistic framework for assessing spatio-temporal point patterns in the archaeological record. J. Archaeol. Sci. 37, 1118–1130. https://doi.org/10.1016/j.jas.2009.12.012

Denis, S., 2012. Le débitage laminaire en silex tertiaire Bartonien dans la culture Blicquy/Villeneuve-Saint-Germain, Néolithique ancien: organisation de la production et réseaux de circulation. Bull. De. la Soci. été Pr. éHist. française 109, 121–143.
Denis, S., 2019. Inter-site relationships at the end of the early neolithic in north-western europe, bartonian flint circulation and macro-features matching method. Lithic Technol. 44, 132–152. https://doi.org/10.1080/01977261.2019.1613009
Dubouloz, J., 2003. Datation absolue du premier Néolithique du Bassin parisien: complément et relecture des données RRBP et VSG. Bull. De. la Soci. été Pr. éHist. française 100, 671–689.
Ducke, B., Suchowska, P., 2022. Exploratory network reconstruction with sparse archaeological data and XTENT. J. Archaeol. Method Theory 29, 508–539. https://doi.org/10.1007/s10816-021-09529-3
Fabrício Machado, A., Miranda, F.R., 2022. The potential distribution of *Cyclopes didactylus*, a silky anteater, reveals a likely unknown population and urgent need for forest conservation in Northeast Brazil. J. Trop. Ecol. 38, 454–461. https://doi.org/10.1017/S0266467422000372
Fjellström, M., Seitsonen, O., Wallén, H., 2022. Mobility in Early Reindeer Herding. In: Salmi, A.-K. (Ed.), Domestication in Action. Springer International Publishing, Cham, pp. 187–212. https://doi.org/10.1007/978-3-030-98643-8_7
Fromont, N., 2013. Anneaux et cultures du néolithique ancien: production, circulation et utilisation entre massifs ardennais et armoricain. BAR International series. Archaeopress, Oxford, England.
Fromont, N., Constantin, C., Vanguestaine, M., 2008. L'apport du site d'Irchonwelz à l'étude de la production des anneaux en schiste blicquiens (Néolithique ancien, Hainaut, Belgique), in: Fin Des Traditions Danubiennes Dans Le Néolithique Du Bassin Parisien (5100-4700 Av. J.-C). Autour Des Recherches de Claude Constantin, Mémoires de La SPF. Société préhistorique française et Presses Universitaires de Namur, Paris, Namur, pp. 425-446.
Furholt, M., 2018. Translocal communities – exploring mobility and migration in sedentary societies of the european neolithic and early bronze age. Praehist. Z. 92, 304–321. https://doi.org/10.1515/pz-2017-0024
Grandell, J., 1976. Doubly Stochastic Poisson Processes, Lecture Notes in Mathematics. Springer Berlin Heidelberg, Berlin, Heidelberg. https://doi.org/10.1007/BFb0077758
GRASS Development Team, 2020. Geographic Resources Analysis Support System (GRASS) Software, Version 7.8.4. Open Source Geospatial Foundation. 〈https://grass.osgeo.org〉.
Hachem, L., Bedault, L., Denis, S., Fromont, N., Hamon, C., Maigrot, Y., Meunier, K., Pernaud, J.-M., 2021. Tinqueux "la Haubette" (Marne, France): un site exceptionnel du néolithique ancien. Archaeopress, Oxford.
Hamon, C., Manen, C., 2021. The mechanisms of neolithisation of western europe: beyond a south/north approach. Open Archaeol. 7, 718–735. https://doi.org/10.1515/opar-2020-0164
Hauzeur, A., 2008. Céramique et Périodisation: Essai de Sériation Du Corpus Blicquien de La Culture de Blicquy/Villeneuve-Saint-Germain, in: Fin Des Traditions Danubiennes Dans Le Néolithique Du Bassin Parisien (5100-4700 Av. J.-C). Autour Des Recherches de Claude Constantin, Mémoires de La SPF. Société préhistorique française et Presses Universitaires de Namur, Paris, Namur, pp. 129-142.
Herzog, I., 2020. Spatial analysis based on cost functions. In: Gillings, M., Hacigüzeller, P., Lock, G. (Eds.), Archaeological Spatial Analysis: A Methodological Guide to GIS. Taylor & Francis Group, London and New York, pp. 333–358.
Herzog, I., 2022. Issues in replication and stability of least-cost path calculations. SDH 5, 131–155. https://doi.org/10.14434/sdh.v5i2.33796
Hijmans, R.J., 2023. terra: Spatial Data Analysis. R package.
Howey, M.C.L., 2007. Using multi-criteria cost surface analysis to explore past regional landscapes: a case study of ritual activity and social interaction in Michigan, AD 1200–1600. J. Archaeol. Sci. 34, 1830–1846. https://doi.org/10.1016/j.jas.2007.01.002
Howey, M.C.L., 2011. Multiple pathways across past landscapes: circuit theory as a complementary geospatial method to least cost path for modeling past movement. J. Archaeol. Sci. 38, 2523–2535. https://doi.org/10.1016/j.jas.2011.03.024
Ilett, M., 2010. Le Néolithique ancien dans le nord de la France, in: La France Préhistorique. Paris, pp. 281–307.
Jadin, I., Verniers, J., 1998. Contribution à l'étude des bracelets du groupe de Blicquy/Villeneuve-Saint-Germain. Approche micropaléontologique et pétrographique des anneaux en schiste du secteur blicquien de Darion. Bull. Des. Cherch. De. la Wallonie 38, 93–109.
Kempf, M., 2021. Take a seed! Revealing Neolithic landscape and agricultural development in the Carpathian Basin through multivariate statistics and environmental modelling. PLoS ONE 16, e0258206. https://doi.org/10.1371/journal.pone.0258206
Kempf, M., Günther, G., 2023. Point pattern and spatial analyses using archaeological and environmental data – a case study from the Neolithic Carpathian Basin. J. Archaeol. Sci.: Rep. 47, 103747. https://doi.org/10.1016/j.jasrep.2022.103747
Lanchon, Y., 2008. La Culture de Blicquy/Villeneuve-Saint-Germain Dans La Basse Vallée de La Marne: Première Approche Chronologique à Partir de La Céramique, in: Fin Des Traditions Danubiennes Dans Le Néolithique Du Bassin Parisien (5100-4700 Av. J.-C). Autour Des Recherches de Claude Constantin, Mémoires de La SPF. Société préhistorique française et Presses Universitaires de Namur, Paris, Namur, pp. 143-159.
Lewis, J., 2021. Probabilistic modelling for incorporating uncertainty in least cost path results: a postdictive roman road case study. J. Archaeol. Method Theory 28, 911–924. https://doi.org/10.1007/s10816-021-09522-w
Lewis, J., 2023b. Explaining known past routes, underdetermination, and the use of multiple cost functions. J. Archaeol. Method Theory. https://doi.org/10.1007/s10816-023-09621-w
Lewis, J., 2023a. leastcostpath: Modelling Pathways and Movement Potential Within a Landscape.
Novaline Jaga, R.M., Sundaram, A., Natarajan, T., 1993. Wasteland development using Geographic Information System techniques. Int. J. Remote Sens. 14, 3249–3257. https://doi.org/10.1080/01431169308904439
Orton, C.R., 1982. Stochastic process and archaeological mechanism in spatial analysis. J. Archaeol. Sci. 9, 1–23. https://doi.org/10.1016/0305-4403(82)90002-4
Pebesma, E., 2018. Simple features for R: standardized support for spatial vector data. R. J. 10, 439. https://doi.org/10.32614/RJ-2018-009
Pebesma, E., Bivand, R., 2023. Spatial Data Science: With Applications in R, 1st ed. Chapman and Hall/CRC, New York. https://doi.org/10.1201/9780429459016
Pétrequin, P., Errera, M., Pétrequin, A.M., Allard, P., 2006. The neolithic quarries of mont viso, piedmont, italy: initial radiocarbon dates. Eur. J. Archaeol., vol. 9 (1), 7–30. https://doi.org/10.1177/1461957107077703
Plateaux, M., 1990. Quelques données sur l'évolution des industries du Néolithique danubien de la vallée de l'Aisne, in: Rubané et Cardial. Néolithique Ancien En Europe Moyenne, Actes Du Colloque International, Liège 1988, ERAUL. Liège, pp. 239–255.
Plateaux, M., 1993. Les industries lithiques du Néolithique danubien dans la vallée de l'Aisne: principes d'analyse en contexte détritique, in: Le Néolithique Au Quotidien, Actes Du XVIe Colloque Interrégional Sur Le Néolithique, Paris, 5–6 Nov.1989. Documents d'Archéologie Française. Maison des Sciences de l'Homme, Paris, pp. 195–206.
Praud, I., Le Gall, J., Vachard, D., 2003. Les bracelets en pierre du Néolithique ancien: provenance et diffusion des matériaux sur les sites Villeneuve-Saint-Germain du Bassin parisien, in: Préhistoire de l'Europe. Des Origines à l'Age Du Bronze. Comité des travaux historiques et scientifiques, pp. 491–502.
Praud, I., Bostyn, F., Cayol, N., Dietsch-Sellami, M.-F., Hamon, C., Lanchon, Y., Vandamme, N., 2018. Les premières occupations du Néolithique ancien dans le Nord-Ouest de La France. Gall. Pr. éHist. 58, 139–215. https://doi.org/10.4000/galliap.891
R Core Team, 2021. R: A language and environment for statistical computing. R Foundation for Statistical Computing, Vienna, Austria. 〈https://www.R-project.org/〉.
Renfrew, C., 1984. Approaches to social archaeology. Harvard University Press, Cambridge, Mass.
Verhagen, P., Jeneson, K., 2012. A Roman Puzzle: Trying to Find the Via Belgica with GIS. In: Thinking Beyond the Tool: Archaeological Computing and the Interpretive Process, BAR International Serie 2344. BAR Publishing, Oxford, pp. 123–130.
White, D.A., Barber, S.B., 2012. Geospatial modeling of pedestrian transportation networks: a case study from precolumbian Oaxaca, Mexico. J. Archaeol. Sci. 39, 2684–2696. https://doi.org/10.1016/j.jas.2012.04.017